hep-th/0110136
MRI-P-011002
PSU/TH-247
NSF-ITP-01-159

Oscillator Representation of the BCFT Construction of D-branes in Vacuum String Field Theory

Partha Mukhopadhyay

Harish-Chandra Research Institute[1]
Chhatnag Road, Jhusi, Allahabad 211019, INDIA

and

Department of Physics
Penn State University
University Park, PA 16802, USA
e-mail: partha@mri.ernet.in, partha@phys.psu.edu

Abstract

Starting from the boundary CFT definition for the D-branes in vacuum string field theory (VSFT) given in hep-th/0105168, we derive the oscillator expression for the D24-brane solution in the VSFT on D25-brane. We show that the state takes the form of a squeezed state, similar to the one found directly in terms of the oscillators and reported in hep-th/0102112. Both the solutions are actually one parameter families of solutions. We also find numerical evidence that at least for moderately large values of the parameter (b) in the oscillator construction the two families of solutions are same under a suitable redefinition of the parameter. Finally we generalize the method to computing the oscillator expression for a D-brane solution with constant gauge field strength turned on along the world volume.

[1]Formerly Mehta Research Institute of Mathematics and Mathematical Physics

Contents

1 Introduction **2**

2 Review of the oscillator and BCFT construction of the D-brane solutions **4**

2.1 Oscillator description of the D-brane solutions 5

2.2 BCFT construction of the D-brane solutions 7

3 Oscillator expression for D24-brane solution in BCFT construction **8**

4 Numerical results **14**

4.1 Determination of $\epsilon(b)$ 14

4.2 Verifying eqs. (**??**) and (**??**) 15

4.3 Verifying the normalization 26

5 Generalization to Neumann-Dirichlet mixed boundary condition **26**

6 Discussion **28**

A Proof of eq.(??) **32**

B Correlation functions with $\sigma^{\pm}(\pm t_0)$ **33**

1 Introduction

Since it was realized [1] that a string field theory [2, 3] can provide a useful setup for the study of Sen's conjectures, much work has taken place to prove the conjectures using Witten's cubic string field theory (CSFT)[2] in the context of bosonic open string theory. A large body of numerical work [4, 5, 6, 7, 8, 9, 10, 11, 12, 13, 14, 15, 16, 17, 18, 19, 20, 21, 22, 23] has verified the conjectures to high accuracy and helped gathering experience on CSFT itself.

Very recently, mainly to understand the part of the conjectures involving the nonexistence of the physical open string excitations around the tachyon vacuum, Rastelli, Sen and Zwiebach (RSZ) started the programme of attacking the problem analytically[24, 25, 26, 27]. In this work[24] they conjectured a simple form for the CSFT expanded around the tachyon vacuum, although it could not be derived from first principles because of the

lack of knowledge of the vacuum solution in an analytic form. This new string field theory which has been called vacuum string field theory (VSFT) in the literature, possesses exactly the same structure as CSFT with the only exception that the BRST operator Q_B in the original CSFT is now replaced by an unknown operator $\mathcal{Q}$ depending only on the ghost part of the theory[2]. Various important algebraic equations in CSFT take the same form in VSFT with Q_B replaced by $\mathcal{Q}$ and hence VSFT has the same gauge invariance and equation of motion as that of CSFT with Q_B replaced by $\mathcal{Q}$.

This work was followed by another[25] by the same authors where the matter parts of various classical solutions of VSFT on D25 brane were constructed using the oscillator language with an ansatz of factorization between the ghost and matter parts. Since these are lump solutions of various codimensions and they produce the expected ratio of tensions of D-branes to a reasonable numerical accuracy, the solutions were interpreted as D-branes of various world volume dimensions. Each of these solutions (except for the one with zero codimension representing the D25 brane itself) is labelled by a continuous parameter b. This has been interpreted to be a gauge parameter, which means that all the solutions in each one parameter family are actually gauge transforms of each other. Existence of these solutions gave the RSZ conjecture a strong foundation.

After this, various works[26, 28, 29] have been done towards finding the multi-D-brane solutions in VSFT. But in the present paper we will be interested in the recent work[27] by RSZ where a different construction of the D-brane solutions in any VSFT has been given through a boundary conformal field theory (BCFT) prescription. BCFT techniques have been used to show that the solutions really satisfy the VSFT equation of motion. In this approach the matter part of any D-brane solution in the VSFT on that D-brane itself is the matter part of the sliver (which is a surface state) [10, 25, 26, 27] corresponding to the relevant BCFT. The matter part of any other D-brane solution has been given as the matter part of a surface-like state where certain boundary condition changing twist operators appear in the correlation functions defining the state. The points of insertions of these operators involve a continuous parameter ϵ. It has been shown in ref.[27] that the states satisfy the desired equation of motion and produce the correct ratio of tensions for an arbitrary positive value of ϵ. Hence it has been interpreted as a gauge parameter like b in the oscillator solutions.

In this work we will be interested in finding the connection between the two one

[2]The operator Q_B being unknown reflects the fact that the complete vacuum solution in CSFT is lacking.

parameter families of solutions corresponding to a D24-brane in the VSFT on D25-brane. For this we first find the oscillator expression for the solution described through BCFT construction[27]. The state takes the form of a squeezed state, - same structure as the one found in oscillator description[25]. Moreover we find numerical evidence that the two families of solutions are actually same with ϵ being a specific function of b. Our computational method relies heavily on the application of Wick's theorem which holds as long as the boundary condition on the fields is linear. We also indicate that the same method can be applied to find the solution for a D-brane with constant gauge field strength turned on along the world volume.

The organization of the paper is as follows: In sec.2 we review the oscillator and BCFT constructions of the D-brane solutions in the VSFT on D25-brane. For the sake of simplicity we will restrict ourselves to the solution of D24-brane placed at the origin with the 25th direction being transverse to the brane. In sec.3 we will start from the BCFT construction of the solution describing the same D24-brane and derive its oscillator expression. In sec.4 we will present the numerical result showing that the ϵ and b-families of solutions are same with ϵ being a specific function of b for moderately large values of b, namely $10 - 25$. In sec.5 we will discuss the more generic situation where a constant gauge field strength is turned on along the world volume. We discuss some numerical issues especially for small values of b in sec.6. Here we show some numerical features which imply that the solutions might be same even for smaller values of b. Some of the computational details are given in the appendices.

2 Review of the oscillator and BCFT construction of the D-brane solutions

Let us start with the classical equation of motion in VSFT.

$$\mathcal{Q}|\Psi\rangle + |\Psi * \Psi\rangle = 0. \tag{2.1}$$

where the string field Ψ is a ghost number 1 state in the Hilbert space (denoted $\mathcal{H}_{BCFT}$) of the combined matter-ghost boundary conformal field theory corresponding to the D-brane on which the string field theory is considered. The full BCFT can be written in the following way:

$$BCFT = (BCFT)_m \oplus (BCFT)_g \,, \tag{2.2}$$

where the subscripts m and g refer to matter and ghost respectively. $(BCFT)_g$ is the usual bc CFT on the upper half plane with central charge -26. This part is universal in the sense that boundary conditions of the ghost fields is same for all the D-branes. $(BCFT)_m$ is the direct sum of 26 CFT's on the upper half plane, each consisting of a single scalar field with boundary condition depending on the D-brane considered. $\mathcal{Q}$ which replaces the BRST charge Q_B in the original CSFT, depends purely on the ghost operators. The star product $A * B$ has its usual meaning.

The factorization ansatz: The factorization ansatz[25] for the D-brane solutions to the above equation reads,

$$|\Psi\rangle = |\Psi_g\rangle \otimes |\Psi_m\rangle, \tag{2.3}$$

where $|\Psi_g\rangle$ depends only on the ghosts and is common to all the D-brane solutions. $|\Psi_m\rangle$ is the matter part which varies for different D-branes.

There is an ambiguity in fixing the overall normalizations of $|\Psi_g\rangle$ and $|\Psi_m\rangle$. This can be fixed by demanding that the factorized equations of motion take the following forms[25]:

$$\mathcal{Q}|\Psi_g\rangle = -|\Psi_g *^g \Psi_g\rangle, \tag{2.4}$$

$$|\Psi_m\rangle = |\Psi_m *^m \Psi_m\rangle, \tag{2.5}$$

where $*^g$ and $*^m$ denote respectively the ghost and matter parts of the star product. Although the normalizations of the ghost and matter parts can diverge or become zero because of the expected appearance of the conformal anomaly while performing computations in either the ghost or the matter conformal field theory, the full solution is expected to be well-behaved.

Here we will be concerned only with eq.(2.5), the solutions to which have been found in ref.[25, 26, 27, 28]. Below we will consider the VSFT on D25 brane and discuss the D24-brane solution in oscillator[25] and BCFT[27] language.

2.1 Oscillator description of the D-brane solutions

We will start with the space-time independent solution[4, 25] corresponding to the D25-brane. This is given by,

$$|\Psi_m\rangle = \mathcal{N}^{26} \exp\left(-\frac{1}{2}\eta_{\mu\nu} \sum_{m,n\geq 1} S_{mn} a_m^{\mu\dagger} a_n^{\nu\dagger}\right) |0_{26}\rangle. \tag{2.6}$$

Here we have adopted the same notation of ref.[25] except for the state $|0_{26}\rangle$. This is the SL(2,R) invariant vacuum which corresponds to the zero value for the 26-dimensional momentum. In this notation a state $|0_n\rangle$ is normalized as follows: $\langle 0_n|0_n\rangle = \frac{V^{(n)}}{(2\pi)^n}$, $V^{(n)}$ being the volume of the n-dimensional Minkowski space. The normalization constant $\mathcal{N}$ and the infinite dimensional matrix S are given by the following relations[25]:

$$\begin{aligned}
\mathcal{N} &= \det(1-X)^{1/2}\det(1+T)^{1/2}, \quad S = CT, \\
T &= \frac{1}{2X}\left(1+X-\sqrt{(1+3X)(1-X)}\right), \\
X &= CV^{11}, \quad C_{mn} = (-1)^m\delta_{mn}.
\end{aligned} \tag{2.7}$$

Here V^{11} is one of the infinite dimensional matrices V^{rs} with $r,s = 1,2,3$[30, 31, 32, 25] that appear in the three-string vertex in the oscillator formalism. For definition and important algebraic properties of these matrices the reader is referred to [25].

Let us now consider the D24-brane solution placed at the origin with x^{25} as the transverse coordinate. The state looks exactly like the state in eq.(2.6) for the tangential directions as $(BCFT)_m$ is the decoupled theory of 26 scalar fields. The $X \equiv X^{25}$ part will now have momentum dependence. The solution takes the following form:

$$|\Psi'_m(b)\rangle = \mathcal{N}^{25}\exp\left(-\frac{1}{2}\eta_{\bar{\mu}\bar{\nu}}\sum_{m,n\geq 1} S_{mn}a_m^{\bar{\mu}\dagger}a_n^{\bar{\nu}\dagger}\right)|0_{25}\rangle \otimes |\Psi'_X(b)\rangle, \tag{2.8}$$

where $\bar{\mu},\bar{\nu} = 0,1\cdots 24$ and,

$$|\Psi'_X(b)\rangle = \mathcal{N}'\exp\left(-\frac{1}{2}\sum_{m,n\geq 0} S'_{mn}a_m^\dagger a_n^\dagger\right)|\Omega_b\rangle, \tag{2.9}$$

where the zero mode oscillator is defined through:

$$a_0 = \frac{\sqrt{b}}{2}\hat{p} \; - \; \frac{i}{\sqrt{b}}\hat{x}, \qquad a_0^\dagger = \frac{\sqrt{b}}{2}\hat{p} \; + \; \frac{i}{\sqrt{b}}\hat{x}. \tag{2.10}$$

Here we have suppressed the superscript "25" for the 25-th direction. b is an arbitrary real number. The constant $\mathcal{N}'$ and the infinite dimensional matrix S' are given as follows[25]:

$$\mathcal{N}' = \frac{\sqrt{3}}{(2\pi b^3)^{1/4}} \left(V_{00}^{rr} + \frac{b}{2}\right) \{\det(1-X')^{1/2} \det(1+T')^{1/2}\},$$
$$S' = C'T', \quad T' = \frac{1}{2X'} \left(1 + X' - \sqrt{(1+3X')\,(1-X')}\right),$$
$$X' = C'V'^{11}(b), \quad C'_{mn} = (-1)^m \delta_{mn}, \quad V_{00}^{rr} = \ln(27/16). \tag{2.11}$$

$V'^{rs}(b)$ are the b dependent matrices introduced in ref.[25] which have the similar algebraic properties as V^{rs} matrices. The relation between the $\hat{p}$ eigenstate and the normalized zero mode harmonic oscillator ground state $|\Omega_b\rangle$ is given by:

$$|p\rangle = (2\pi/b)^{-1/4} \ \exp\left[-\frac{b}{4}\, p^2 \ + \ \sqrt{b}\, p\, a_0^\dagger \ - \ \frac{1}{2}\left(a_0^\dagger\right)^2\right] |\Omega_b\rangle. \tag{2.12}$$

Using this relation one can express eq.(2.9) in terms of the momentum eigenstates. It takes the following form:

$$|\Psi'_X(b)\rangle = \int dp\ h(p,b)\ \exp\left(-\frac{1}{2}\, a^\dagger.Q(b).a^\dagger \ + \ p\ L(b).a^\dagger\right)\ |p\rangle, \tag{2.13}$$

where,

$$\begin{aligned}
Q_{mn}(b) &= S'_{mn} \ + \ \frac{S'_{0m}S'_{0n}}{(1-S'_{00})}, && \forall m,n \geq 1,\\
L_n(b) &= -\frac{\sqrt{b}S'_{0n}}{1-S'_{00}}, && \forall n \geq 1,\\
h(p,b) &= (2\pi/b)^{-1/4}\ (1-S'_{00})^{-1/2}\mathcal{N}' \exp\left(-\frac{B}{2}p^2\right),\\
B &= b\left(\frac{1}{2} \ + \ \frac{S'_{00}}{1-S'_{00}}\right).
\end{aligned} \tag{2.14}$$

2.2 BCFT construction of the D-brane solutions

In ref.[27] the D-brane solutions of a VSFT have been constructed using the BCFT description. In this approach every D-brane solution is described by the sliver $|\Xi_{BCFT}\rangle$ of the corresponding BCFT. An open string field theory is always defined on a particular D-brane. Let us denote the BCFT and the state space corresponding to this reference D-brane by $BCFT$ and $\mathcal{H}_{BCFT}$ respectively. Now if $BCFT'$ and $\mathcal{H}_{BCFT'}$ denote respectively the BCFT and the state space corresponding to the D-brane for which the solution

is sought, then the matter part of the solution is given by the matter part of $|\Xi_{BCFT'}\rangle$ expressed in $\mathcal{H}_{BCFT}$ [3]. The prescription for expressing $|\Xi_{BCFT'}\rangle$ in $\mathcal{H}_{BCFT}$ is given by giving the BPZ inner product of $|\Xi_{BCFT'}\rangle$ with an arbitrary state in $\mathcal{H}_{BCFT}$. This is given by the following correlator on the UHP [27]:

$$\langle \Xi_{BCFT'}|\phi\rangle = (2\epsilon)^{2h} \left\langle f\circ\phi(0)\ \sigma^+\left(\frac{\pi}{4}+\epsilon\right)\sigma^-\left(-\frac{\pi}{4}-\epsilon\right)\right\rangle_{BCFT}, \quad |\phi\rangle \in \mathcal{H}_{BCFT}, \tag{2.15}$$

where $\sigma^+(t)$ ($t\in\mathbf{R}$) is the vertex operator of the ground state of string with its left end (if viewed from inside the UHP) on the $BCFT'$-brane and right end on the $BCFT$-brane. Similarly $\sigma^-(t)$ is the ground state vertex operator for the string connecting the two branes in the opposite orientation. These operators[4] are dimension h primaries which change the boundary condition respectively from $BCFT$ to $BCFT'$ and $BCFT'$ to $BCFT$ on the real line. Therefore the above notation means that the correlator has to be computed with $BCFT$ boundary condition for $|t|\leq(\frac{\pi}{4}+\epsilon)$ and $BCFT'$ boundary condition on the rest of the real line. ϵ is an arbitrary real positive parameter. $\phi(t)$ is the vertex operator for the state $|\phi\rangle$ and $f\circ\phi(t)$ denotes the transformation of $\phi(t)$ under the following conformal map:

$$f(z) = \tan^{-1}(z). \tag{2.16}$$

In case $BCFT'$ and $BCFT$ are same, $\sigma^\pm$ become the identity operator with $h=0$ and the above definition reduces to the usual definition of the sliver [27].

It has been demonstrated in ref.[27] that $|\Xi_{BCFT'}\rangle$ $*$-multiplies to itself for any ϵ. From the definition (2.15) it is clear that $|\Xi_{BCFT'}\rangle$ factorizes into ghost and matter parts since $\sigma^\pm$ do not involve any ghost part. But again the ambiguity of normalization is obvious. The normalization can be fixed by demanding that the matter part $*$-multiplies to itself:

$$|\Xi_{BCFT'_m}\rangle *^m |\Xi_{BCFT'_m}\rangle = |\Xi_{BCFT'_m}\rangle. \tag{2.17}$$

$|\Xi_{BCFT'_m}\rangle$ defined in this way is conjectured to be the matter part of the $BCFT'$-brane solution.

[3] Note that $|\Xi_{BCFT'}\rangle$ is originally a state in $\mathcal{H}_{BCFT'}$.

[4] For a systematic study of the correlation functions in presence of the σ operators in case of only Neumann and Dirichlet boundary conditions and for more references on this subject see ref.[33].

3 Oscillator expression for D24-brane solution in BCFT construction

Here we will use the prescription (2.15) to find the oscillator expression for the D24-brane solution in the VSFT formulated on D25-brane. The D24-brane will be placed at the origin with x^{25} as the transverse direction. Therefore in our analysis $BCFT$ will correspond to the D25-brane and $BCFT'$ to the D24-brane. For notational simplicity we will denote $|\Xi_{BCFT}\rangle$ by $|\Xi\rangle$ and $|\Xi_{BCFT'}\rangle$ by $|\Xi'\rangle$.

The first step in our computation will be to find the BCFT construction for the matter part of $BCFT'$ sliver i.e. $|\Xi'_m\rangle$. It is given by a prescription similar to that in eq.(2.15) with $\phi \in \mathcal{H}_{BCFT_m}$. The only difference is that, now there is an unknown overall constant which is so adjusted that $|\Xi'_m\rangle$ (and hence also $|\Xi'_g\rangle$) $*$-multiplies [5] to itself. Therefore,

$$\langle \Xi'_m|\phi\rangle = \widehat{\mathcal{N}}^{26}(2\epsilon)^{2h}\left\langle f\circ\phi(0)\ \sigma^+\left(\frac{\pi}{4}+\epsilon\right)\sigma^-\left(-\frac{\pi}{4}-\epsilon\right)\right\rangle_{BCFT_m}, \qquad |\phi\rangle \in \mathcal{H}_{BCFT_m}. \tag{3.1}$$

$\widehat{\mathcal{N}}$ can be found a follows. Since $|\Xi'_g\rangle \otimes |\Xi'_m\rangle$ is given by eq.(2.15), $|\Xi'_g\rangle$ will have a normalization constant $\widehat{\mathcal{N}}^{-26}$. On the other hand $|\Xi'_g\rangle$ and $|\Xi_g\rangle$ are identical, and hence $|\Xi_m\rangle$ must have the same normalization constant $\widehat{\mathcal{N}}^{26}$.

$$\langle \Xi_m|\phi\rangle = \widehat{\mathcal{N}}^{26}\langle f\circ\phi(0)\rangle_{BCFT_m}, \qquad |\phi\rangle \in \mathcal{H}_{BCFT_m}. \tag{3.2}$$

It can be proved (see end of this section) that $|\Xi_m\rangle$ with the above definition has the following oscillator expression:

$$|\Xi_m\rangle = \widehat{\mathcal{N}}^{26}\exp\left(-\frac{1}{2}\eta_{\mu\nu}\sum_{m,n\geq 1}\widehat{S}_{mn}a_m^{\mu\dagger}a_n^{\nu\dagger}\right)|0_{26}\rangle, \tag{3.3}$$

where $\widehat{S}_{mn}$'s are given as follows [25],

$$\widehat{S}_{mn} \;=\; -\frac{1}{\sqrt{mn}}\oint\frac{dz}{2\pi i}\oint\frac{dw}{2\pi i}\,(\tan z)^{-m}\,(\tan w)^{-n}\,(z-w)^{-2}. \tag{3.4}$$

It was argued with numerical results in ref.[25] that (see eqs.(2.6), (2.7))

$$\widehat{\mathcal{N}} = \mathcal{N}, \qquad \widehat{S}_{mn} = S_{mn}. \tag{3.5}$$

[5] Note that the star product of $|\Xi'_m\rangle$ can not be computed using the nice geometrical arguments used in ref.[27] because of the conformal anomaly coming from the nonzero central charge of $BCFT_m$.

Thus,

$$\langle \Xi'_m|\phi\rangle = \mathcal{N}^{26}(2\epsilon)^{2h}\left\langle f\circ\phi(0)\ \sigma^+\left(\frac{\pi}{4}+\epsilon\right)\sigma^-\left(-\frac{\pi}{4}-\epsilon\right)\right\rangle_{BCFT_m}, \qquad |\phi\rangle\in\mathcal{H}_{BCFT_m}. \tag{3.6}$$

Now the difference between $BCFT$ and $BCFT'$ comes only from the world-sheet field $X = X^{25}$ as this is the only one which has N-D boundary condition. All the other matter fields are N-N. Therefore only X can see the presence of $\sigma^\pm$ and it acts as the identity operator for all the other matter fields. Hence $|\Xi'_m\rangle$ looks exactly like $|\Xi_m\rangle$ for the excitations along $X^0,\cdots,X^{24}$. Therefore,

$$|\Xi'_m(\epsilon)\rangle = \mathcal{N}^{25}\exp\left(-\frac{1}{2}\eta_{\bar\mu\bar\nu}\sum_{m,n\geq 1}S_{mn}a_m^{\bar\mu\dagger}a_n^{\bar\nu\dagger}\right)|0_{25}\rangle\otimes|\Xi'_X(\epsilon)\rangle, \tag{3.7}$$

where $|\Xi'_X(\epsilon)\rangle$ is defined through the following relation:

$$\begin{aligned}\langle\Xi'_X(\epsilon)|\phi\rangle &= \mathcal{N}\ (2\epsilon)^{2h}\langle f\circ\phi(0)\ \sigma^+(t_0)\ \sigma^-(-t_0)\rangle_{BCFT_X}, \qquad |\phi\rangle\in\mathcal{H}_{BCFT_X},\\ t_0 &= \frac{\pi}{4}+\epsilon.\end{aligned} \tag{3.8}$$

Hence at this stage our job is to find the oscillator expression for $|\Xi'_X(\epsilon)\rangle$ and compare it with eq.(2.13). To this end we find it useful to define[6] the following generating function,[7]

$$G(j,p,t_0)\equiv\langle f\circ\exp(j.a^\dagger)\ e^{ipX}(0)\ \sigma^+(t_0)\ \sigma^-(-t_0)\rangle, \tag{3.9}$$

where $j.a^\dagger=\sum_{n\geq 1}j_na_n^\dagger$ and j_n's are real numbers. $f\circ\exp(j.a^\dagger)$ is defined as follows. The residue expression for the creation operators in the $\alpha'=1$ unit is given by:

$$a_n^\dagger = \frac{1}{\sqrt{2n}}\oint\frac{dw}{2\pi}\ w^{-n}\ \partial X(w). \tag{3.10}$$

Now applying the technique of ref.[34, 35] we get,

$$f\circ a_n^\dagger = \frac{1}{\sqrt{2n}}\oint\frac{dz}{2\pi}\ \left(f^{-1}(z)\right)^{-n}\ \partial X(z). \tag{3.11}$$

Then we define $f\circ\exp(j.a^\dagger)$ through the power series expansion of the exponential.

$$f\circ\exp(j.a^\dagger)=\sum_{N\geq 0}\frac{1}{N!}\left[j.\left(f\circ a^\dagger\right)\right]^N. \tag{3.12}$$

[6] We thank Justin David for his suggestion on this issue.

[7] This point onwards we will suppress the subscript "$BCFT_X$" in the correlation function for notational simplicity.

The use of $G(j,p,t_0)$ lies in the fact that it directly gives the oscillator expression for $|\Xi'_X\rangle$ through the following prescription (see appendix A for a proof):

$$|\Xi'_X(\epsilon)\rangle = \mathcal{N}\ (2\epsilon)^{2h}\ \int dp\ G(j_n\ \rightarrow (-1)^{n+1}\ a_n^\dagger, -p, t_0)\ |p\rangle, \tag{3.13}$$

where $G(j_n \rightarrow (-1)^{n+1}a_n^\dagger, -p, t_0)$ in the above expression means that j_n is replaced by $(-1)^{n+1}\ a_n^\dagger$ in the expression of $G(j,-p,t_0)$ after its computation is over. Therefore our next job will be to compute the generating function $G(j,p,t_0)$.

Computation of $G(j,p,t_0)$: Our approach of computing $G(j,p,t_0)$ will be to find a first order differential equation of $G(j,p,t_0)$ with respect to j_n and then integrate it. Let us start by expanding $\exp(j.a^\dagger)$ in eq.(3.9)

$$\begin{aligned}
G(j,p,t_0) &= \sum_{N=0}^{\infty}\ \frac{1}{N!}\ \langle (j.f\circ a^\dagger)^N\ e^{ipX}(0)\ \sigma^+(t_0)\ \sigma^-(-t_0)\rangle \\
&= \sum_{N=0}^{\infty}\ \frac{1}{N!}\sum_{\{n_i\}}\prod_{i=1}^{N}\Big(j_{n_i}\langle f\circ a_{n_i}^\dagger\ e^{ipX}(0)\ \sigma^+(t_0)\ \sigma^-(-t_0)\rangle\Big) \\
&= \sum_{N=0}^{\infty}\frac{1}{N!}\sum_{\{n_i\}}\prod_{i=1}^{N}\left(\frac{j_{n_i}}{\sqrt{2n_i}}\right)\oint\ \prod_{i=1}^{N}\left[\frac{dz_i}{2\pi}\ (\tan z_i)^{-n_i}\right] \\
&\quad \langle\prod_{i=1}^{N}\partial X(z_i)\ e^{ipX}(0)\ \sigma^+(t_0)\ \sigma^-(-t_0)\rangle,
\end{aligned} \tag{3.14}$$

where in the last step we have used eq.(3.11) with $f^{-1}(z) = \tan z$. Similarly the first order derivative with respect to j_m takes the following form:

$$\begin{aligned}
\partial_{j_m}G(j,p,t_0) &= \sum_{N=0}^{\infty}\frac{1}{N!}\sum_{\{n_i\}}\prod_{i=1}^{N}\left(\frac{j_{n_i}}{\sqrt{2n_i}}\right)\frac{1}{\sqrt{2m}}\oint\ \prod_{i=1}^{N}\left[\frac{dz_i}{2\pi}\ (\tan z_i)^{-n_i}\right] \\
&\quad \oint\frac{dz}{2\pi}\ (\tan z)^{-m}\langle\partial X(z)\prod_{i=1}^{N}\partial X(z_i)\ e^{ipX}(0)\rangle_{\sigma(t_0)},
\end{aligned} \tag{3.15}$$

where we have used the following notation: $\langle\cdots\rangle_{\sigma(t_0)} \equiv \langle\cdots\sigma^+(t_0)\ \sigma^-(-t_0)\rangle$. Now our aim will be to extract the z dependence of the above correlation function so that the z integral can finally be taken out of all the summations. This could be done by computing the full correlation function. But we find it easier to do the computation in a different way. Our aim is to express the right hand side in such a way that it has $G(j,p,t_0)$ as a factor. Once it is done we can do the integration quite easily. This will be achieved by explicitly writing the result of contracting only $\partial X(z)$ with the other fields and leaving

the other parts uncontracted[8]. Doing this we get,

$$\langle \partial X(z) \prod_{i=1}^{N} \partial X(z_i)\ e^{ipX}(0)\rangle_{\sigma(t_0)} \;=\; \sum_{k=1}^{N} T_2(z,z_k,t_0)\ \langle \prod_{i\neq k}^{N} \partial X(z_i)\ e^{ipX}(0)\rangle_{\sigma(t_0)} + ip\ T_1(z,t_0)\ \langle \prod_{i=1}^{N} \partial X(z_i)\ e^{ipX}(0)\rangle_{\sigma(t_0)}. \quad (3.16)$$

Here,

$$T_2(z,z_k,t_0) \equiv \partial_z \partial_{z_k} \mathcal{G}^N(z,z_k,t_0), \qquad T_1(z,t_0) \equiv \partial_z \mathcal{G}^N(z,0,t_0) \quad (3.17)$$

are the results of contracting $\partial X(z)$ with $\partial X(z_k)$ and $X(0)$ respectively. $\mathcal{G}^N$ is an effective normalized two point function defined through[9],

$$\mathcal{G}^N(z,w,t_0) \;\equiv\; \frac{\langle X(z)\ X(w)\ \sigma^+(t_0)\ \sigma^-(-t_0)\rangle}{\langle \sigma^+(t_0)\ \sigma^-(-t_0)\rangle}. \quad (3.18)$$

Using eq.(3.16) in eq.(3.15) one gets,

$$\begin{aligned}
&\partial_{j_m} G(j,p,t_0) \\
&= \sum_{N=1}^{\infty} \frac{1}{N!} \sum_{k=1}^{N} \left\{ \sum_{n_k=1}^{\infty} \frac{j_{n_k}}{\sqrt{2n_k}} \frac{1}{\sqrt{2m}} \oint \frac{dz}{2\pi} \frac{dz_k}{2\pi}\ (\tan z)^{-m}\ (\tan z_k)^{-n_k} T_2(z,z_k,t_0) \right\} \\
&\left\{ \sum_{\{n_i\}_{i\neq k}} \prod_{i\neq k}^{N} \left(\frac{j_{n_i}}{\sqrt{2n_i}} \right) \oint \prod_{i\neq k}^{N} \left[\frac{dz_i}{2\pi}\ (\tan z_i)^{-n_i} \right]\ \langle \prod_{i\neq k}^{N} \partial X(z_i)\ e^{ipX}(0)\rangle_{\sigma(t_0)} \right\} \\
&+ \frac{ip}{\sqrt{2m}} \left(\oint \frac{dz}{2\pi}\ (\tan z)^{-m}\ T_1(z,t_0) \right)\ G(j,p,t_0), \qquad (3.19)
\end{aligned}$$

where in the last line we have made use of eq.(3.14). The summand of the k summation has two parts which are kept in two pairs of curly brackets in the first two lines. The k dependence of the quantity in the first pair of curly brackets comes only through n_k and z_k both of which are summed over. Hence it is k independent. For the second part also the k dependence is only formal, as we can just remove it by renaming n_i by n_{i-1} for $i \geq k$. Therefore finally we get,

[8]This can only be done in cases where Wick's theorem holds. Although the presence of σ operators means that the boundary theory is interacting we will explicitly show in appendix B that Wick'e theorem actually holds, but with an effective normalized two point function.

[9]The details of calculations of the correlators in presence of the σ operators [33] will be presented in appendix B.

$$\begin{aligned}
\partial_{j_m} G(j,p,t_0) &= \Bigg[-\sum_{n=1}^{\infty} \frac{j_n}{2\sqrt{mn}} \oint \frac{dz}{2\pi i}\frac{dw}{2\pi i} (\tan z)^{-m} (\tan w)^{-n} T_2(z,w,t_0) \\
&\quad + \frac{ip}{\sqrt{2m}} \oint \frac{dz}{2\pi} (\tan z)^{-m} T_1(z,t_0) \Bigg] G(j,p,t_0) \\
&= \left[-\sum_{n\geq 1} \widehat{Q}_{mn}\, j_n \;+\; p\, \widetilde{L}_m \right] G(j,p,t_0), \qquad (3.20)
\end{aligned}$$

where,

$$\begin{aligned}
\widehat{Q}_{mn}(\epsilon) &= \frac{1}{2\sqrt{mn}} \oint \frac{dz}{2\pi i} \oint \frac{dw}{2\pi i} (\tan z)^{-m} (\tan w)^{-n} \partial_z \partial_w \mathcal{G}^N(z,w,t_0), \\
\widetilde{L}_n(\epsilon) &= -\frac{1}{\sqrt{2n}} \oint \frac{dz}{2\pi i} (\tan z)^{-n} \partial_z \mathcal{G}^N(z,0,t_0). \qquad (3.21)
\end{aligned}$$

Note that we have used the definitions (3.17). $\widehat{Q}_{mn}$ and $\widetilde{L}_n$ are considered to be functions of ϵ as $t_0 = \pi/4 + \epsilon$. Now integrating eq.(3.20) for all values of m we get,

$$G(j,p,t_0) = G(0,p,t_0)\, \exp\left(-\frac{1}{2}\, j.\widehat{Q}(\epsilon).j \;+\; p\; j.\widetilde{L}(\epsilon) \right), \qquad (3.22)$$

where $G(0,p,t_0) = \langle e^{ipX}(0)\rangle_{\sigma(t_0)}$ is the constant of integration. Now using eqs.(3.13) and (3.22) one can express $|\Xi'_X(\epsilon)\rangle$ in terms of $\mathcal{G}^N$ and $\langle e^{ipX}(0)\rangle_{\sigma(t_0)}$:

$$\begin{aligned}
|\Xi'_X(\epsilon)\rangle &= \oint dp\;\; \widehat{h}(p,\epsilon)\; \exp\left(-\frac{1}{2}\, a^\dagger.\widehat{Q}(\epsilon).a^\dagger \;+\; p\; \widehat{L}(\epsilon).a^\dagger \right) |p\rangle, \\
\widehat{L}_n(\epsilon) &= (-1)^n\, \widetilde{L}_n(\epsilon), \\
\widehat{h}(p,\epsilon) &= \mathcal{N}\, (2\epsilon)^{2h}\, \langle e^{-ipX}(0)\rangle_{\sigma(t_0)}. \qquad (3.23)
\end{aligned}$$

To complete the derivation one needs to know the expressions for $\mathcal{G}^N(z,w,t_0)$ and $\langle e^{ipX}(0)\rangle_{\sigma(t_0)}$. Borrowing the results from appendix B (eqs.(B.13, B.15, B.25)) we get,

$$\begin{aligned}
\widehat{Q}_{mn}(\epsilon) &= \frac{1}{\sqrt{mn}} \oint \frac{dz}{2\pi i} \oint \frac{dw}{2\pi i} (\tan z)^{-m} (\tan w)^{-n} (z-w)^{-2} \\
&\qquad\qquad (t_0^2 - z^2)^{-1/2} (t_0^2 - w^2)^{-1/2} (zw - t_0^2), \\
\widehat{L}_n(\epsilon) &= (-1)^n \sqrt{\frac{2}{n}}\; t_0 \oint \frac{dz}{2\pi i} (\tan z)^{-n}\; z^{-1}\; (t_0^2 - z^2)^{-1/2},
\end{aligned}$$

$$\widehat{h}(p,\epsilon) \;=\; \mathcal{N}\;\left(1+\frac{\pi}{4\epsilon}\right)^{-1/8}\;\;\left(2\epsilon+\frac{\pi}{2}\right)^{-p^2}. \tag{3.24}$$

Therefore $|\Xi'_X(\epsilon)\rangle$ has the same form as $|\Psi'_X(b)\rangle$ (eq.(2.13)). It is also clear that ϵ plays the role similar to b. Now the question is how these two states are related. Surprisingly, we find numerical evidence that $|\Xi'_X(\epsilon)\rangle$ is the same one parameter family of states as $|\Psi'_X(b)\rangle$ with ϵ being a suitable function of b. We will present these results in the next section.

Before ending this section we will briefly indicate how one derives the expressions in eqs. (3.3) and (3.4) using the method described above. The definition (3.2) can be considered to be the special case of eq.(3.1) where $\sigma^{\pm}$ = identity and $h = 0$. Using this and following the similar derivation given in appendix A it is straightforward to show that the analog of eq.(3.13) reads,

$$|\Xi_X\rangle = \widehat{\mathcal{N}}\;\int dp\; G(j_n\;\rightarrow\;(-1)^{n+1}a_n^\dagger, -p)\;|p\rangle, \tag{3.25}$$

where,

$$G(j,p) \equiv \langle f\circ\exp(j.a^\dagger)\;e^{ipX}(0)\rangle. \tag{3.26}$$

Clearly the correlation function has to be computed in the BCFT of D25-brane. Proceeding in the same way as discussed in this section one gets,

$$G(j,p) = \delta(p)\;\exp\left(-\frac{1}{2}\;j.\widehat{S}.j\right), \tag{3.27}$$

where $\widehat{S}_{mn}$'s are given by eq.(3.4) which is same as $\widehat{Q}_{mn}$ given in eqs.(3.21) with $\partial_z\partial_w\mathcal{G}^N(z,w,t_0)$ replaced by $\langle\partial X(z)\;\partial X(w)\rangle = -2(z-w)^{-2}$ (see eq.(B.3)). This result along with eq.(3.25) and the fact that with BCFT corresponding to the D25-brane all the directions should look the same, immediately justifies eq.(3.3).

4 Numerical results

To show that $|\Xi'_X(\epsilon)\rangle$ and $|\Psi'_X(b)\rangle$ are actually the same family of solutions we need to establish that the following relations are true with some suitable function $\epsilon(b)$:

$$\widehat{Q}_{mn}(\epsilon) \;=\; Q_{mn}(b), \qquad \forall m,n\geq 1, \tag{4.1}$$

$$\widehat{L}_n(\epsilon) \;=\; L_n(b), \qquad \forall n\geq 1, \tag{4.2}$$

$$\widehat{h}(p,\epsilon) \;=\; h(p,b). \tag{4.3}$$

In the following we will perform partial numerical verification of the above equations.

4.1 Determination of $\epsilon(b)$

To verify eqs. (4.1) and (4.2) one needs to know $\epsilon(b)$ which we determine by equating the widths of the gaussians $\widehat{h}(p,\epsilon)$ and $h(p,b)$ as functions of p. We get the following relation:

$$\epsilon = \frac{1}{2}\exp\left[\frac{b}{2}\left(\frac{1}{2}+\frac{S'_{00}}{1-S'_{00}}\right)\right] \;-\; \frac{\pi}{4} \tag{4.4}$$

ϵ in the definition (2.15), is a real positive parameter. Hence the two solutions (2.13) and (3.23) can coincide only in the range $0 \leq \epsilon < \infty$. Numerically this range corresponds to

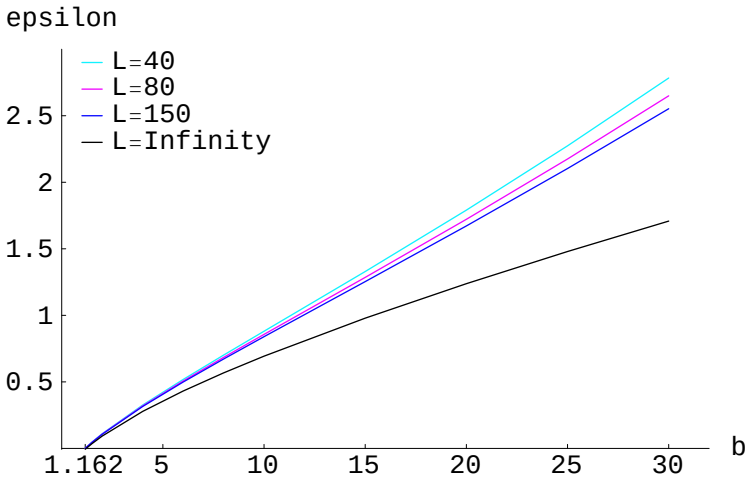

Figure 1: Numerical plot of $\epsilon(b)$ for $L = 40,\ 80,\ 150,\ \infty$. The $L = \infty$ curve has been obtained by extrapolating the numerical data with the help of a fit of the form: $a_0 + a_1/\log(L) + a_2/(\log(L))^2$.

$b_0 \leq b < \infty$, where $b_0 \equiv b(\epsilon = 0)$. We have performed numerical computations only up to $L = 150$. At this level we find $\epsilon(b = 1.16243) = 3.86646 \times 10^{-7}$. We have displayed in fig.1, the numerical plot of the function $\epsilon(b)$ up to $b = 30$ for $L = 40,\ 80,\ 150$ and ∞.

It can be shown that ϵ diverges as b goes to infinity. For this one uses the large b dependence of S'_{00} (see eq.(4.4)). Using the expression for the matrix S' given in eqs.(2.11) and the b dependent matrices $V'^{rs}(b)$ given in ref.[25] one can show: $\lim_{b\to\infty} S'_{00} \to -1$. Numerically we find the following large b behaviour of S'_{00} (see fig.2):

$$S'_{00} \sim -1 + c.b^{-1/2} + \mathcal{O}(b^{-1}), \tag{4.5}$$

where c is a positive constant, determined numerically to be around 2.23 (fig.2) at $L = 150$. Using this expansion in eq.(4.4) it is easy to show:

$$\lim_{b\to\infty} \epsilon \to \infty \tag{4.6}$$

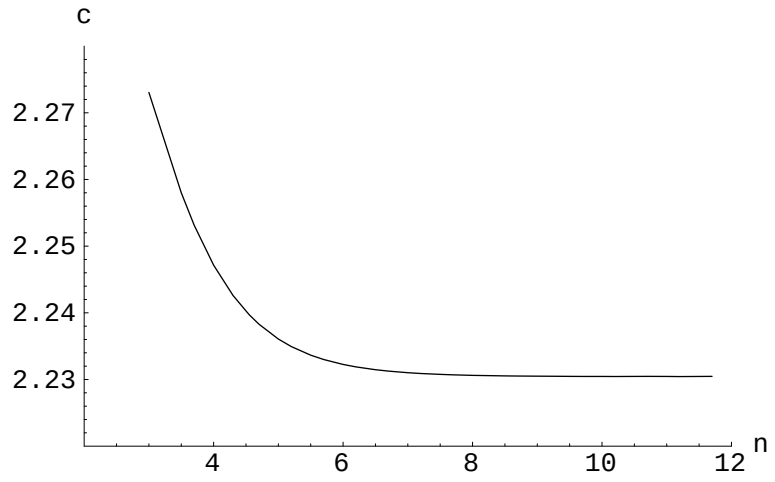

Figure 2: Plot of $c = b^{1/2}(S'_{00} + 1)$ against n, where $n = \log_{10} b$. $L = 150$ result.

4.2 Verifying eqs. (4.1) and (4.2)

Using the functional relation (4.4) we check eqs.(4.1) and (4.2) for a few values of m and n. We present these numerical results in tables 1, 2, $\cdots$, 18. In these tables we have displayed the difference between l.h.s. and r.h.s. of eqs. (4.1) and (4.2) computed in level truncation. Here "level truncation" carries the usual meaning. We have performed the computations at a variety of values of b, namely 10, 15, 20 and 25 up to level $L = 150$. At each level we have displayed the value of the percentage deviation P_{mn} or P_n defined through:

$$P_{mn} \equiv 100 \left(\frac{\widehat{Q}_{mn} - Q_{mn}}{Q_{mn}} \right), \qquad P_n \equiv 100 \left(\frac{\widehat{L}_n - L_n}{L_n} \right). \tag{4.7}$$

In the cases where magnitude of the percentage deviation is around 20 or more at $L = 20$, we have extrapolated the result to $L = \infty$ by using a fit of the form:

$$a_0 \ + \ a_1 \left(\frac{1}{\log L} \right) \ + \ a_2 \left(\frac{1}{\log L} \right)^2 .$$

The numerical results show that typically P_{mn} or P_n approaches monotonically to zero as L increases when respectively $|\widehat{Q}_{mn} - Q_{mn}|$ or $|\widehat{L}_n - L_n| \geq 10^{-2}$ at $L = 20$. The monotonic nature is absent when $|\widehat{Q}_{mn} - Q_{mn}|$ or $|\widehat{L}_n - L_n| \approx 10^{-3}$ at $L = 20$. But in these cases $(\widehat{Q}_{26} - Q_{26})$ itself is very small so that the numerical values are not quite reliable. There is only one exceptional case, namely Q_{24} at $b = 10$, where although $|\widehat{Q}_{24} - Q_{24}| = 0.004610$ at $L = 20$, P_{24} decreases monotonically as L increases. It should be emphasized here that neither of Q_{mn} and $\widehat{Q}_{mn}$ can be computed exactly. Q_{mn} is always computed in level truncation and here $\widehat{Q}_{mn}$ also depends[10] on the level as it uses the function $\epsilon(b)$ (eq.(4.4)) which is evaluated in level truncation. One can check from fig.1 that $\epsilon(b)$ depends reasonably on L.

[10]This is also true for $\widehat{L}_n$.

b	10			15		
L	Q_{11}	$\widehat{Q}_{11} - Q_{11}$	P_{11}	Q_{11}	$\widehat{Q}_{11} - Q_{11}$	P_{11}
20	0.095904	0.063869	66.57	0.14419	0.083102	57.65
40	0.097524	0.05576	57.18	0.1467	0.07485	51.02
60	0.098219	0.051846	52.79	0.14779	0.070844	47.94
80	0.098626	0.049385	50.07	0.14844	0.06831	46.02
100	0.098901	0.04764	48.17	0.14888	0.066506	44.67
150	0.099324	0.044774	45.08	0.149558	0.063539	42.48
∞	0.103999	0.004353	4.19	0.157412	0.021230	13.49

Table 1: Numerical check of eq.(4.1) for $(m, n) = (1, 1)$ at $b = 10,\ 15$ in level truncation.

b	20			25		
L	Q_{11}	$\widehat{Q}_{11} - Q_{11}$	P_{11}	Q_{11}	$\widehat{Q}_{11} - Q_{11}$	P_{11}
20	0.17272	0.090202	52.22	0.191686	0.092387	48.2
40	0.17592	0.082084	46.66	0.195448	0.084469	43.22
60	0.17733	0.078135	44.06	0.197114	0.080619	40.9
80	0.17817	0.075634	42.45	0.198111	0.07818	39.46
100	0.17875	0.073848	41.31	0.198794	0.076437	38.45
150	0.179641	0.070906	39.47	0.199866	0.073563	36.81
∞	0.19031	0.004162	2.19	0.212775	0.001696	0.80

Table 2: Numerical check of eq.(4.1) for $(m, n) = (1, 1)$ at $b = 20,\ 25$ in level truncation.

b	10			15		
L	Q_{13}	$\widehat{Q}_{13} - Q_{13}$	P_{13}	Q_{13}	$\widehat{Q}_{13} - Q_{13}$	P_{13}
20	-0.064555	-0.015287	23.68	-0.079509	-0.022967	28.89
40	-0.066134	-0.011948	18.07	-0.081656	-0.018588	22.76
60	-0.066822	-0.010416	15.59	-0.0826	-0.016532	20.01
80	-0.067226	-0.009481	14.1	-0.083160	-0.015261	18.35
100	-0.067499	-0.008832	13.08	-0.083541	-0.014369	17.2
150	-0.067919	-0.007798	11.48	-0.084131	-0.012931	15.37
∞	-0.072715	0.005613	-7.72	-0.072715	0.006507	-8.95

Table 3: Numerical check of eq.(4.1) for $(m, n) = (1, 3)$ at $b = 10,\ 15$ in level truncation.

b	20			25		
L	Q_{13}	$\widehat{Q}_{13} - Q_{13}$	P_{13}	Q_{13}	$\widehat{Q}_{13} - Q_{13}$	P_{13}
20	-0.08850	-0.029099	32.88	-0.094546	-0.033075	34.98
40	-0.091064	-0.024321	26.71	-0.097428	-0.028163	28.91
60	-0.092202	-0.022054	23.92	-0.098716	-0.025820	26.16
80	-0.092880	-0.020643	22.22	-0.099487	-0.024358	24.48
100	-0.093342	-0.019648	21.05	-0.100015	-0.023324	23.32
150	-0.094064	-0.018035	19.17	-0.100841	-0.021641	21.46
∞	-0.102734	0.004162	-4.05	-0.110942	0.001696	-1.53

Table 4: Numerical check of eq.(4.1) for $(m, n) = (1, 3)$ at $b = 20,\ 25$ in level truncation.

b	10			15		
L	Q_{15}	$\widehat{Q}_{15} - Q_{15}$	P_{15}	Q_{15}	$\widehat{Q}_{15} - Q_{15}$	P_{15}
20	0.044457	0.009871	22.20	0.053378	0.014552	27.26
40	0.045886	0.007425	16.18	0.055269	0.011262	20.38
60	0.046518	0.006305	13.55	0.056114	0.009726	17.33
80	0.046892	0.005625	12.00	0.056617	0.008783	15.51
100	0.047145	0.005155	10.93	0.056959	0.008125	14.26
150	0.047535	0.004410	9.28	0.057491	0.007071	12.30
∞	0.052152	-0.005177	-9.93	0.063944	-0.006995	-10.94

Table 5: Numerical check of eq.(4.1) for $(m, n) = (1, 5)$ at $b = 10,\ 15$ in level truncation.

b	20			25		
L	Q_{15}	$\widehat{Q}_{15} - Q_{15}$	P_{15}	Q_{15}	$\widehat{Q}_{15} - Q_{15}$	P_{15}
20	0.058778	0.018997	32.32	0.062426	0.022237	35.62
40	0.061002	0.015290	25.06	0.064899	0.018345	28.27
60	0.062003	0.013539	21.84	0.066019	0.016493	24.98
80	0.062601	0.012455	19.90	0.066692	0.015342	23.00
100	0.063010	0.011695	18.56	0.067153	0.014531	21.64
150	0.063649	0.010469	16.45	0.067875	0.013220	19.48
∞	0.071531	-0.006240	-8.72	0.076923	-0.004874	-6.34

Table 6: Numerical check of eq.(4.1) for $(m, n) = (1, 5)$ at $b = 20,\ 25$ in level truncation.

b	10			15		
L	Q_{22}	$\widehat{Q}_{22} - Q_{22}$	P_{22}	Q_{22}	$\widehat{Q}_{22} - Q_{22}$	P_{22}
20	-0.079754	-0.001975	2.48	-0.075862	0.003572	-4.71
40	-0.082366	-0.000510	0.61	-0.078173	0.005258	-6.73
60	-0.083606	0.000145	0.17	-0.079263	0.006018	-7.59
80	-0.084373	0.000534	-0.63	-0.079936	0.006473	-8.10
100	-0.084912	0.000798	-0.94	-0.080406	0.006784	-8.44
150	-0.085779	0.001207	-1.41	-0.081162	0.007267	-8.95

Table 7: Numerical check of eq.(4.1) for $(m, n) = (2, 2)$ at $b = 10,\ 15$ in level truncation.

b	20			25		
L	Q_{22}	$\widehat{Q}_{22} - Q_{22}$	P_{22}	Q_{22}	$\widehat{Q}_{22} - Q_{22}$	P_{22}
20	-0.073516	0.004370	-5.94	-0.071926	0.004047	-5.63
40	-0.075639	0.006135	-8.11	-0.073918	0.005825	-7.88
60	-0.076635	0.006937	-9.05	-0.074848	0.006636	-8.87
80	-0.077247	0.007419	-9.60	-0.075419	0.007125	-9.45
100	-0.077675	0.007749	-9.98	-0.075817	0.007462	-9.84
150	-0.078360	0.008267	-10.55	-0.076452	0.007991	-10.45

Table 8: Numerical check of eq.(4.1) for $(m, n) = (2, 2)$ at $b = 20,\ 25$ in level truncation.

b	10			15		
L	Q_{24}	$\widehat{Q}_{24} - Q_{24}$	P_{24}	Q_{24}	$\widehat{Q}_{24} - Q_{24}$	P_{24}
20	0.053782	0.004610	8.57	0.051590	0.000756	1.47
40	0.055938	0.003106	5.55	0.053533	-0.000742	-1.39
60	0.056966	0.002403	4.22	0.054455	-0.001432	-2.63
80	0.057602	0.001976	3.43	0.055023	-0.001848	-3.36
100	0.058048	0.001681	2.90	0.055420	-0.002133	-3.85
150	0.058763	0.001215	2.07	0.056055	-0.002581	-4.60

Table 9: Numerical check of eq.(4.1) for $(m, n) = (2, 4)$ at $b = 10,\ 15$ in level truncation.

b	20			25		
L	Q_{24}	$\widehat{Q}_{24} - Q_{24}$	P_{24}	Q_{24}	$\widehat{Q}_{24} - Q_{24}$	P_{24}
20	0.050262	-0.000283	-0.56	0.049358	-0.000410	-0.83
40	0.052071	-0.001809	-3.47	0.051073	-0.001947	-3.81
60	0.052925	-0.002512	-4.75	0.051880	-0.002655	-5.12
80	0.053450	-0.002935	-5.49	0.052374	-0.003083	-5.89
100	0.053815	-0.003226	-5.99	0.052718	-0.003376	-6.40
150	0.054399	-0.003681	-6.77	0.053265	-0.003837	-7.20

Table 10: Numerical check of eq.(4.1) for $(m, n) = (2, 4)$ at $b = 20,\ 25$ in level truncation.

b	10			15		
L	Q_{26}	$\widehat{Q}_{26} - Q_{26}$	P_{26}	Q_{26}	$\widehat{Q}_{26} - Q_{26}$	P_{26}
20	-0.040383	-0.005042	12.48	-0.038843	-0.002041	5.25
40	-0.042280	-0.003613	8.54	-0.040566	-0.000666	1.64
60	-0.043194	-0.002932	6.79	-0.041393	-0.000021	00.05
80	-0.043761	-0.002514	5.74	-0.041904	0.000372	-00.89
100	-0.044159	-0.002224	5.04	-0.042261	0.000643	-1.52
150	-0.044796	-0.001764	3.94	-0.042832	0.001068	-2.49

Table 11: Numerical check of eq.(4.1) for $(m, n) = (2, 6)$ at $b = 10,\ 15$ in level truncation.

b	20			25		
L	Q_{26}	$\widehat{Q}_{26} - Q_{26}$	P_{26}	Q_{26}	$\widehat{Q}_{26} - Q_{26}$	P_{26}
20	-0.037906	-0.001058	2.79	-0.037268	-0.000820	2.20
40	-0.039521	0.000322	-8.15	-0.038806	0.000564	-1.45
60	-0.040292	0.000967	-2.40	-0.039537	0.001211	-3.06
80	-0.040766	0.001359	-3.33	-0.039987	0.001603	-4.01
100	-0.041098	0.001628	-3.96	-0.040300	0.001874	-4.65
150	-0.041626	0.002051	-4.93	-0.040798	0.002298	-5.63

Table 12: Numerical check of eq.(4.1) for $(m, n) = (2, 6)$ at $b = 20,\ 25$ in level truncation.

b	10			15		
L	L_2	$\widehat{L}_2 - L_2$	P_2	L_2	$\widehat{L}_2 - L_2$	P_2
20	-0.364194	-0.128913	35.40	-0.392023	-0.168603	43.01
40	-0.373869	-0.112747	30.16	-0.402758	-0.152126	37.77
60	-0.378499	-0.1049	27.72	-0.407913	-0.144056	35.32
80	-0.381390	-0.099956	26.21	-0.41114	-0.138943	33.80
100	-0.383433	-0.096438	25.15	-0.413425	-0.135291	32.72
150	-0.386752	-0.090679	23.45	-0.417147	-0.129283	30.99
∞	-0.432994	-0.008689	2.01	-0.469289	-0.042665	9.09

Table 13: Numerical check of eq.(4.2) for $n = 2$ at $b = 10,\ 15$ in level truncation.

b	20			25		
L	L_2	$\widehat{L}_2 - L_2$	P_2	L_2	$\widehat{L}_2 - L_2$	P_2
20	-0.410521	-0.185730	45.25	-0.424065	-0.193342	45.59
40	-0.421957	-0.169384	40.14	-0.436008	-0.177242	40.65
60	-0.427461	-0.161341	37.74	-0.441764	-0.169302	38.32
80	-0.430911	-0.156229	36.26	-0.445377	-0.164248	36.88
100	-0.433357	-0.15257	35.21	-0.447939	-0.160625	35.86
150	-0.437346	-0.146534	33.50	-0.452121	-0.154641	34.20
∞	-0.493419	-0.058952	11.95	-0.511047	-0.067541	13.22

Table 14: Numerical check of eq.(4.2) for $n = 2$ at $b = 20,\ 25$ in level truncation.

b	10			15		
L	L_4	$\widehat{L}_4 - L_4$	P_4	L_4	$\widehat{L}_4 - L_4$	P_4
20	0.197429	0.079438	40.24	0.213512	0.106990	50.11
40	0.205318	0.067864	33.05	0.222368	0.094046	42.29
60	0.209112	0.062277	29.78	0.226643	0.087723	38.71
80	0.211479	0.058776	27.79	0.229317	0.083734	36.51
100	0.213150	0.056297	26.41	0.231207	0.080895	34.99
150	0.215855	0.052265	24.21	0.234277	0.076248	32.55
∞	0.253767	- 0.004626	- 1.82	0.277538	0.009568	3.45

Table 15: Numerical check of eq.(4.2) for $n = 4$ at $b = 10,\ 15$ in level truncation.

b	20			25		
L	L_4	$\widehat{L}_4 - L_4$	P_4	L_4	$\widehat{L}_4 - L_4$	P_4
20	0.224276	0.123145	54.91	0.232196	0.132486	57.06
40	0.233791	0.109760	46.95	0.242196	0.119019	49.14
60	0.238393	0.103176	43.28	0.247042	0.112367	45.48
80	0.241277	0.099004	41.03	0.250081	0.108141	43.24
100	0.243318	0.096025	39.46	0.252233	0.105119	41.68
150	0.246636	0.091132	36.95	0.255736	0.100143	39.16
∞	0.293560	0.020229	6.89	0.305394	0.027642	9.05

Table 16: Numerical check of eq.(4.2) for $n = 4$ at $b = 20,\ 25$ in level truncation.

b	10			15		
L	L_6	$\widehat{L}_6 - L_6$	P_6	L_6	$\widehat{L}_6 - L_6$	P_6
20	-0.135727	-0.061953	45.65	-0.147193	-0.083386	56.65
40	-0.142626	-0.052404	36.74	-0.154976	-0.072390	46.71
60	-0.145976	-0.04777	32.72	-0.158771	-0.066998	42.20
80	-0.148072	-0.044866	30.30	-0.161150	-0.063595	39.46
100	-0.149551	-0.042811	28.63	-0.162832	-0.061177	37.57
150	-0.151945	-0.039472	25.98	-0.165562	-0.057225	34.56
∞	-0.18594	0.007933	-4.27	-0.204543	-0.000255	0.12

Table 17: Numerical check of eq.(4.2) for $n = 6$ at $b = 10,\ 15$ in level truncation.

b	20			25		
L	L_6	$\widehat{L}_6 - L_6$	P_6	L_6	$\widehat{L}_6 - L_6$	P_6
20	-0.154897	-0.097548	62.98	-0.160580	-0.106541	66.35
40	-0.163288	-0.085937	52.63	-0.169423	-0.094710	55.90
60	-0.167387	-0.080199	47.91	-0.173751	-0.088833	51.13
80	-0.169962	-0.076562	45.05	-0.176472	-0.085097	48.22
100	-0.171785	-0.073968	43.06	-0.178400	-0.082426	46.20
150	-0.174748	-0.069714	39.89	-0.181536	-0.078036	42.99
∞	-0.217198	-0.007736	3.56	-0.226578	-0.013637	6.02

Table 18: Numerical check of eq.(4.2) for $n = 6$ at $b = 20,\ 25$ in level truncation.

4.3 Verifying the normalization

Now one also needs to verify that the normalizations of the gaussians $\widehat{h}(p,\epsilon)$ and $h(p,b)$ match, as we have not checked if $|\Xi'_X(\epsilon)\rangle$ $*$-multiplies to itself separately in the oscillator language. The condition that the normalizations match reads,

$$\begin{aligned} R &\equiv \sqrt{\frac{2\pi b}{3}}\,(V_{00}^{rr}+b/2)^{-1}\,(1-S'_{00})^{1/2}\,\left(1+\frac{\pi}{4\epsilon}\right)^{-1/8}\,\frac{\det(1-X)^{1/2}\det(1+T)^{1/2}}{\det(1-X')^{1/2}\det(1+T')^{1/2}}, \\ &= 1. \end{aligned} \tag{4.8}$$

We present the numerical result for $(1-R)$ in table 19. Here also one notices the same behaviour of the numerical data. $(1-R)$ approaches monotonically to zero as L increases when it is fairly large ($|1-R| \geq 10^{-2}$). When $|1-R| \approx 10^{-3}$ as in the cases of $b=2$ and 6, the behaviour is not that regular.

b / L	2	4	6	8	10	15	20	25
20	-0.003741	-0.014667	0.003411	0.022327	0.039967	0.078096	0.109525	0.136126
40	0.002474	-0.012070	0.003655	0.020720	0.036840	0.072135	0.101614	0.126813
60	0.005389	-0.010920	0.003643	0.019777	0.035123	0.068950	0.097396	0.121839
80	0.007207	-0.010216	0.003599	0.019129	0.033970	0.066828	0.094586	0.118518
100	0.008497	-0.009723	0.003552	0.018643	0.033116	0.065260	0.092506	0.116057
150	0.019609	-0.008923	0.003449	0.017802	0.031650	0.062577	0.088939	0.111827
∞	0.133653	0.000960	0.000114	0.003431	0.007829	0.019969	0.032435	0.044717

Table 19: Numerical values of $(1-R)$ at various values of b in level truncation. The $L=\infty$ results are obtained by extrapolation with a fit of the following form: $a_0 + a_1/\log(L) + a_2/(\log(L))^2$.

5 Generalization to Neumann-Dirichlet mixed boundary condition

Our method of computing the oscillator expression of a D-brane solution in BCFT construction relied mainly on the validity of Wick's theorem. Applicability of Wick's theorem

made it possible to get a simple first order differential equation of $G(j,p,t_0)$ (eq.(3.20)) so that it can be integrated easily. Although the presence of σ operators in the correlation function makes the boundary theory nontrivial, the final action is still quadratic as both the Neumann and Dirichlet boundary conditions connect the normal and tangential derivatives of X on the world-sheet boundary in a linear way. In fact Wick's theorem is expected to be applicable in a more generic situation where the boundary condition involves the vanishing of an arbitrary linear combination of the normal and tangential derivatives. Let us consider the example of a D25-brane solution with a background constant gauge field strength $F_{\mu\nu}$ along the world volume in the VSFT on D25-brane. Here $BCFT$ still corresponds to the usual D25-brane as before but now $BCFT'$ corresponds to the following boundary condition ($z = e^{\tau+i\sigma}$):

$$\partial_\sigma X^\mu(\tau,\sigma) \ + \ \eta^{\mu\nu} \ \Omega_{\nu\gamma}(F) \ \partial_\tau X^\gamma(\tau,\sigma)|_{\sigma=0,\pi} = 0, \tag{5.1}$$

where $\Omega_{\mu\nu}(F)$ is an antisymmetric constant matrix proportional to $F_{\mu\nu}$. In this case one needs to compute the following normalized two point function (see discussion in appendix B) with Neumann boundary condition on $|t| < t_0$ and boundary condition (5.1) on the rest of the real line.

$$\mathcal{G}^{N\mu\nu}(z,w,t_0,F) = \frac{\langle X^\mu(z) \ X^\nu(w)\rangle_{\sigma(t_0)}}{\langle \sigma^+(t_0) \ \sigma^-(-t_0)\rangle}, \tag{5.2}$$

where the σ operators are defined in the same way as before with D.b.c. replaced by eq.(5.1). Just like the usual D25-brane the present solution should also not have any momentum excitation as the full translational invariance is still preserved. Therefore it is sufficient to consider $G(j,0,t_0)$ in this case. Using the same method that was followed in sec.3 one can show that the solution (denoted $|\Xi_F\rangle$)is given by the following:

$$|\Xi_F\rangle = \exp\left(-\frac{1}{2}\sum_{m,n\geq 1} \widehat{Q}_{\mu\nu mn}(\epsilon,F) \ a_m^{\mu\dagger} a_n^{\nu\dagger}\right)|0_{26}\rangle, \tag{5.3}$$

where,

$$\widehat{Q}_{\mu\nu mn}(\epsilon,F) = \frac{1}{2\sqrt{mn}} \ \oint \frac{dz}{2\pi i} \ \frac{dw}{2\pi i} \ (\tan z)^{-m} \ (\tan w)^{-n} \ \partial_z\partial_w \mathcal{G}^N_{\mu\nu}(z,w,t_0,F). \tag{5.4}$$

If we consider a lower dimensional brane solution then the transverse directions simply corresponds to D.b.c. and hence each of them looks the same as that found in sec.3.

6 Discussion

1. We have found numerical evidence that the two states $|\Psi'_X(b)\rangle$ (eq.(2.13)) and $|\Xi'_X(\epsilon)\rangle$ (eqs.(3.8)) are same with a specific relation (eq.(4.4)) between the respective gauge parameters b and ϵ for a moderately large values of b, namely $10 - 25$.

   Here we will try to partially investigate the case of smaller values of b . We find that the numerical agreement is not good for smaller values of b if we follow the same method as that used in sec.4 to compare the two states. For example, we find $P_{11} = 75.9$ for $b = 4$. It may be possible that the two solutions are different for small values of ϵ. But comparing the two states in a different manner we again get good numerical agreement. In the following we will elaborate on this issue.

   Comparing the two solutions involve checking the conditions (4.1), (4.2) and (4.3) which give a set of infinite number of equations. One needs to choose only one of them to fix the function $\epsilon(b)$ and verify the rest of the infinite number of equations using that function. The numerical result will certainly depend on the specific equation chosen to determine $\epsilon(b)$. In fact the numerical accuracy to which a specific equation belonging to the set $\{(4.1), (4.2), (4.3)\}$ is satisfied for a certain value of b will depend on this choice. In sec.4, we have fixed the function $\epsilon(b)$ by equating (eq.(4.4)) the widths of the gaussians $\widehat{h}(p, \epsilon)$ and $h(p, b)$. It may happen that this is not a good choice for $b < 10$ at least for those equations which are not satisfied very well numerically, for example eq.(4.1) for $(m, n) = (1, 1)$ (as it gives $P_{11} = 75.9$). In that case some different choice should improve the numerical result. In the following we will give an example to demonstrate this.

   In fig.3 we have plotted $\widehat{Q}_{11}$ against b using the level 150 results. We see that $\widehat{Q}_{11}$ is reasonably flat for $b > 10$. The slope of the curve increases gradually below $b = 10$ and it becomes considerably large below $b = 5$. Since $\epsilon(b)$ is almost linear (fig.1) for such values of b at $L = 150$, the slope of $\widehat{Q}_{11}$ with respect to ϵ also becomes larger below $b = 10$. This means that small error in computing ϵ induces large error in the value of $\widehat{Q}_{11}$. This could be the possible reason for getting unsatisfactory numerical results for small b. To check if it is true one can perform the numerical verification in the opposite order, i.e. first use the following equation to determine $t_0 = (\epsilon + \pi/4)$ (see eqs. (2.14) and (3.24)) as a function of b,

$$\widehat{Q}_{11}(\epsilon) = Q_{11}(b), \tag{6.1}$$

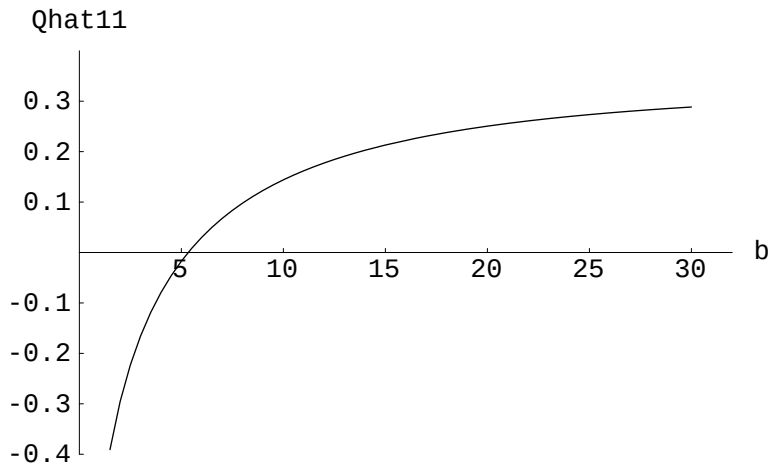

Figure 3: Plot of $\widehat{Q}_{11}$ against b. $L = 150$ result.

then check if the following equation (condition for the equality of widths - eq.(4.4)) is satisfied:

$$t_0 = \frac{1}{2} \exp\left[\frac{b}{2}\left(\frac{1}{2} \; + \; \frac{S'_{00}}{1 - S'_{00}}\right)\right]. \tag{6.2}$$

We have performed computations for $b = 2,\ 4,\ 6,\ 8$ and the numerical results seem to be much better in this case. We have presented these results in tables 20 and 21 where we have used the following notations: t_0^Q is the value of t_0 obtained by solving eq.(6.1) and t_0^{width} is the value of t_0 obtained by evaluating the r.h.s. of eq.(6.2). The percentage deviation P has the following definition:

$$P = 100\left(\frac{t_0^Q \; - \; t_0^{width}}{t_0^Q}\right) \tag{6.3}$$

The $L = \infty$ results are obtained by using the same fit as used earlier in this paper.

2. The numerical estimate of $b_0 = b(\epsilon = 0)$ also changes substantially when one chooses different equations to determine $\epsilon(b)$. For example using eq.(6.1) we find: $\epsilon(b = 1.16243) = 0.117631$, $\epsilon(b = 0.395339) = 9.94763 \times 10^{-8}$. One can argue that b_0 has to be a nonzero positive number in the following way. Numerically ($L = 150$) we find the following small b behaviour of S'_{00}:

$$S'_{00} \sim 1 - 1.083\ b^{1/2} + \mathcal{O}(b). \tag{6.4}$$

b	2			4		
L	t_0^Q	$t_0^Q - t_0^{width}$	P	t_0^Q	$t_0^Q - t_0^{width}$	P
20	0.992418	0.093157	9.39	1.14835	0.02844	2.54
40	0.992437	0.096443	9.72	1.14885	0.03737	3.36
60	0.992446	0.097959	9.87	1.14906	0.04152	3.75
80	0.992452	0.098887	9.96	1.14918	0.04408	3.99
100	0.992456	0.099534	10.03	1.14926	0.04586	4.16
150	0.992461	0.100568	10.13	1.14939	0.04874	4.43
∞	0.99254	0.114123	11.50	1.1507	0.086969	7.56

Table 20: Numerical results for t_0^Q (solution of eq.(6.1) and t_0^{width} (r.h.s. of eq.(6.2) in level truncation at $b = 2,\ 4$.

b	6			8		
L	t_0^Q	$t_0^Q - t_0^{width}$	P	t_0^Q	$t_0^Q - t_0^{width}$	P
20	1.26718	-0.05133	-4.05	1.36587	-0.14333	-10.49
40	1.26873	-0.03493	-2.75	1.36895	-0.1179	-8.61
60	1.2694	-0.02727	-2.15	1.37027	-0.10599	-7.73
80	1.26978	-0.02255	-1.78	1.37104	-0.09862	-7.19
100	1.27004	-0.01923	-1.51	1.37156	-0.09343	-6.81
140	1.27037	-0.01473	-1.16	1.37223	-0.086398	-6.30
∞	1.27472	0.058027	4.55	1.38116	0.028155	2.03

Table 21: Numerical results for t_0^Q (solution of eq.(6.1) and t_0^{width} (r.h.s. of eq.(6.2) in level truncation at $b = 6,\ 8$.

Using this in eq.(4.4) one can show that, $\epsilon(0) = (1/2 - \pi/4) < 0$ which implies that b_0 has to be positive.

3. For $b = 10 - 25$ one could try to fix $\epsilon(b)$ from the normalization (condition (4.8)) and verify if the widths match. This again is not numerically efficient because of the following reason: the ϵ dependence of eq.(4.8) is a factor with a small exponent , namely $\left(1 + \frac{\pi}{4\epsilon}\right)^{-1/8}$. Therefore the other part of the equation which is computed numerically, has to be raised to the 8th power to compute ϵ. This increases the numerical error in the value of ϵ as compared to the one obtained from comparing the widths of the gaussians. Because of the same reason the numerical test of eq.(4.8) is not very much sensitive to the functional relation (4.4).

4. It is interesting that in some cases we get very small numbers even at a low level. For example we get $(\widehat{Q}_{26} - Q_{26}) = -0.003848$ at $L = 6$ (the lowest value that can be chosen for $(m, n) = (2, 6)$) and $b = 25$, $(1 - R) = -0.001445$ at $L = 1$ and $b = 2$. Typically in these cases we see that the quantity does not monotonically converge to zero as we increase level. To understand this situation more one needs to perform computations at higher levels.

5. From table19 we see that the value of $(1 - R)$ at a given level drifts away from zero as we increase b. This indicates the fact that at larger values of b or ϵ the higher levels contribute more. This also happens when ϵ approaches zero as we can see it in the following table ($L = 150$ results):

b	1.7	1.2	1.167	1.16250	1.16243
ϵ	0.070290	5.242×10^{-3}	6.412×10^{-4}	1.02086×10^{-5}	3.86646×10^{-7}
$1 - R$	0.034139	0.258735	0.427176	0.658365	0.773086

Table 22: $L = 150$ results for $(1 - R)$ as ϵ tends to zero.

6. The method of translating the BCFT construction of a D-brane solution to its oscillator description as described in this paper only required a certain normalized two point function with specific boundary conditions on the real line. It will be interesting to explore the higher dimensional D-brane solutions in the VSFT on a

lower dimensional D-brane. For example one may try to see how the D25-brane solution looks in the VSFT on a D24-brane.

A Proof of eq.(3.13)

Let us start from the definition of $|\Xi'_X(\epsilon)\rangle$, namely eq.(3.8). Taking $|\phi\rangle = (a^\dagger_{n_1}\ a^\dagger_{n_2}\cdots)\ |p\rangle$ one can write:

$$\begin{aligned}
&\langle\Xi'_X(\epsilon)|\ (a^\dagger_{n_1}\ a^\dagger_{n_2}\cdots)\ |p\rangle \\
&= \mathcal{N}\ (2\epsilon)^{2h}\ \langle (f\circ a^\dagger_{n_1}\ f\circ a^\dagger_{n_2}\cdots)\ f\circ e^{ipX}(0)\ \sigma^+(t_0)\sigma^-(-t_0)\rangle \\
&= \mathcal{N}\ (2\epsilon)^{2h}\ \langle (f\circ a^\dagger_{n_1}\ f\circ a^\dagger_{n_2}\cdots)\ e^{ipX}(0)\ \sigma^+(t_0)\sigma^-(-t_0)\rangle \\
&= \mathcal{N}\ (2\epsilon)^{2h}\ \left[(\partial_{j_{n_1}}\partial_{j_{n_2}}\cdots)\ G(j,p,t_0)\right]_{j=0}
\end{aligned} \tag{A.1}$$

$|\phi\rangle$ considered above has the generic form of a state in $\mathcal{H}_{BCFT_X}$. Let us now expand $|\Xi'_X(\epsilon)\rangle$ in terms of the basis vectors of this type and take its BPZ conjugate:

$$|\Xi'_X(\epsilon)\rangle \ = \ \sum_{\{N_n\}}\ \int\ dp\ C^{\Xi}_{\{N_n\}}(p,\epsilon)\ \prod_{n=1}^{\infty}\ \left(a^\dagger_n\right)^{N_n}\ |p\rangle, \tag{A.2}$$

$$\langle\Xi'_X(\epsilon)| \ = \ \sum_{\{N_n\}}\ \int\ dp\ C^{\Xi}_{\{N_n\}}(p,\epsilon)\ (-1)^{\sum_n (1+n)N_n}\langle p|\ \prod_{n=1}^{\infty}\ (a_n)^{N_n}\,, \tag{A.3}$$

where, $N_n = 0, 1, \cdots\infty, \forall n \geq 1$. Therefore taking the BPZ inner product with the state $\prod_{n=1}^{\infty}\ \left(a^\dagger_n\right)^{N_n}\ |p\rangle$ one gets:

$$\langle\Xi'_X(\epsilon)|\ \prod_{n=1}^{\infty}\ \left(a^\dagger_n\right)^{N_n}\ |p\rangle = C^{\Xi}_{\{N_n\}}(-p,\epsilon)\ (-1)^{\sum_n (1+n)N_n}\ \prod_{n=1}^{\infty}\ (N_n!)\,. \tag{A.4}$$

The series expansion of $G(j,p,t_0)$ in powers of j_n's will look like,

$$G(j,p,t_0) = \sum_{\{N_n\}} C^{G}_{\{N_n\}}(p,\epsilon)\ \prod_{n=1}^{\infty}\ (j_n)^{N_n}. \tag{A.5}$$

Therefore,

$$\left[\prod_{n=1}^{\infty}\left(\partial^{N_n}_{j_n}\right)\ G(j,p,t_0)\right]_{j=0} = C^{G}_{\{N_n\}}(p,\epsilon)\ \prod_{n=1}^{\infty}\ (N_n!)\,. \tag{A.6}$$

Now using eqs.(A.1, A.4, A.6) one can write,

$$C^{\Xi}_{\{N_n\}}(p,\epsilon) = \mathcal{N}\ (2\epsilon)^{2h}\ (-1)^{\sum_{n=1}^{\infty}(1+n)N_n}\ C^{G}_{\{N_n\}}(-p,\epsilon). \tag{A.7}$$

Using this expression in eq.(A.2) we get,

$$\begin{aligned} |\Xi'_X(\epsilon)\rangle &= \mathcal{N}\ (2\epsilon)^{2h}\ \int\ dp\ \left[\ \sum_{\{N_n\}}\ C^{G}_{\{N_n\}}(-p,\epsilon)\ \prod_{n\geq 1}\ \left((-1)^{1+n}a_n^{\dagger}\right)^{N_n}\right]\ |p\rangle \\ &= \mathcal{N}\ (2\epsilon)^{2h}\ \int\ dp\ G(j_n \to (-1)^{1+n}a_n^{\dagger}, -p, t_0)\ |p\rangle, \end{aligned} \tag{A.8}$$

which is eq.(3.13).

B Correlation functions with $\sigma^{\pm}(\pm t_0)$

As defined in subsection 2.2, $\sigma^{\pm}(t)$ (also called the twist operators in the literature) are the vertex operators of the ground states of strings connecting the Neumann and Dirichlet boundary conditions with opposite orientations. These are primaries with conformal dimension $h = 1/16$ and have the following OPE with ∂X [33]:

$$\partial X(z)\ \sigma^{\pm}(w) = (z-w)^{-1/2}\ \tau^{\pm}(w)\ +\ \text{Reg.}, \tag{B.1}$$

where $\tau^{\pm}(z)$ are the next excited twist fields. We will take the following normalization for $\sigma^{\pm}$:

$$\sigma^{\pm}(z)\ \sigma^{\pm}(w) = (z-w)^{-1/8}\ +\ \text{Reg.} \tag{B.2}$$

Eq.(3.10) and the commutation relation $[a_m, a_n^{\dagger}] = \delta_{mn}$ fix the normalization of ∂X,

$$\partial X(z)\ \partial X(w) = -2\ (z-w)^{-2}\ +\ \text{Reg.} \tag{B.3}$$

Now we will use the above short distance behaviours and the method of analyticity to compute the twisted two point function $g^{(2)} \equiv \langle \partial X(z)\ \partial X(w)\ \sigma^{+}(u)\ \sigma^{-}(v)\rangle$. First of all one notices that the singularities of z as it approaches $w,\ u$ and v are $-2(z-w)^{-2}$, $(z-u)^{-1/2}$ and $(z-v)^{-1/2}$ respectively. Therefore $g^{(2)}$ should take the following form:

$$g^{(2)} = -2(z-w)^{-2}(z-u)^{-1/2}(z-v)^{-1/2}\ \left[f_1(w,u,v)\ +\ z f_2(w,u,v)\ +\ \cdots\right]. \tag{B.4}$$

But the large z behaviour of $g^{(2)}$, namely $\lim_{z\to\infty} z^2 g^{(2)}(z,w,u,v) \to$ finite, truncates the above series at the second term. Therefore we are left with computing the two unknown

functions $f_1(w,u,v)$ and $f_2(w,u,v)$. Now let us focus only on the $z \to w$ behaviour of $g^{(2)}$. Using eqs. (B.2) and (B.3) we get,

$$g^{(2)} = -2(z-w)^{-2}\ (u-v)^{-1/8}\ +\ \text{Reg.} \tag{B.5}$$

Expanding eq.(B.4) in powers of $(z-w)$ we get,

$$\begin{aligned} g^{(2)} \ &= \ -2\ (z-w)^{-2}\left[(w-u)^{-1/2}(w-v)^{-1/2}(f_1+wf_2)\right] \\ &\quad -2\ (z-w)^{-1}\left[(w-u)^{-1/2}(w-v)^{-1/2}\right. \\ &\quad \left.\left(f_2\ -\ \frac{1}{2}(f_1+wf_2)\left[(w-u)^{-1}+(w-v)^{-1}\right]\right)\right]\ +\ \text{Reg.} \end{aligned} \tag{B.6}$$

Matching the coefficients of $(z-w)^{-2}$ and $(z-w)^{-1}$ from eqs. (B.5) and (B.6) we get the following two equations:

$$(f_1+wf_2) \ = \ (w-u)^{1/2}(w-v)^{1/2}(u-v)^{-1/8}, \tag{B.7}$$

$$(f_1+wf_2) \ = \ \frac{2f_2}{(w-u)^{-1}+(w-v)^{-1}}. \tag{B.8}$$

Solving eqs. (B.7) and (B.8) for $f_1(w,u,v)$ and $f_2(w,u,v)$ we get,

$$f_1(w,u,v) \ = \ -(w-u)^{-1/2}(w-v)^{-1/2}(u-v)^{-1/8}\left(\frac{wu}{2}\ +\ \frac{wv}{2}\ -\ uv\right), \tag{B.9}$$

$$f_2(w,u,v) \ = \ \frac{1}{2}(w-u)^{-1/2}(w-v)^{-1/2}(u-v)^{-1/8}\ (2w-u-v). \tag{B.10}$$

Finally substituting this result in eq.(B.4) we get,

$$\begin{aligned} &\langle \partial X(z)\ \partial X(w)\ \sigma^+(u)\ \sigma^-(v)\rangle \\ &= -2\ (z-w)^{-2}\ (z-u)^{-1/2}\ (z-v)^{-1/2}\ (w-u)^{-1/2}\ (w-v)^{-1/2} \\ &\quad (u-v)^{-1/8}\left(zw-\tfrac{1}{2}zu-\tfrac{1}{2}zv-\tfrac{1}{2}wu-\tfrac{1}{2}wv+uv\right). \end{aligned} \tag{B.11}$$

The corresponding normalized correlator would be defined as,

$$\langle \partial X(z)\ \partial X(w)\ \sigma^+(u)\ \sigma^-(v)\rangle^N \equiv \frac{\langle \partial X(z)\ \partial X(w)\ \sigma^+(u)\ \sigma^-(v)\rangle}{\langle \sigma^+(u)\ \sigma^-(v)\rangle}. \tag{B.12}$$

Using eqs.(B.2, B.11, B.12) we get,

$$\begin{aligned} T_2(z,w,t_0) &\equiv \langle \partial X(z)\ \partial X(w)\rangle^N_{\sigma(t_0)} \\ &= \frac{\langle \partial X(z)\ \partial X(w)\ \sigma^+(t_0)\ \sigma^-(-t_0)\rangle}{\langle \sigma^+(t_0)\ \sigma^-(-t_0)\rangle} \\ &= 2\ (z-w)^{-2}\ (t_0^2-z^2)^{-1/2}\ (t_0^2-w^2)^{-1/2}\ (zw-t_0^2). \end{aligned} \tag{B.13}$$

It is straightforward to verify that this is consistent with the following result for the normalized two point function of X obtained by applying the method of images in ref.[36]:

$$\mathcal{G}^N(z,w,t_0) \equiv \langle X(z)\ X(w)\rangle^N_{\sigma(t_0)} = -2\ \ln\left[\frac{1\ -\ \sqrt{\frac{(z\ +\ t_0)(w\ -\ t_0)}{(w\ +\ t_0)(z\ -\ t_0)}}}{1\ +\ \sqrt{\frac{(z\ +\ t_0)(w\ -\ t_0)}{(w\ +\ t_0)(z\ -\ t_0)}}}\right]. \tag{B.14}$$

Now we define,

$$T_1(z,t_0) \equiv \langle \partial X(z)\ X(0)\rangle^N_{\sigma(t_0)} = \partial_z \mathcal{G}^N(z,0,t_0) = -2\ t_0\ z^{-1}\ (t_0^2-z^2)^{-1/2} \tag{B.15}$$

Note that $T_2(z,w,t_0)$ and $T_1(z,t_0)$ defined above have been used in the first two equations of (3.24).

Now we are left with the job of computing $\langle e^{ipX}(0)\rangle_{\sigma(t_0)}$ (the result of which was used in the third equation of (3.24)) and explicitly checking that Wick's theorem really holds. We will do this in the following way. First we will assume that Wick's theorem holds for the normalized correlators and derive the expression for $\langle\prod_{i=1}^M\ e^{ik_iX}(z_i)\rangle^N_{\sigma(t_0)}$ using Wick's theorem and path integral arguments. Then we will show that this result is consistent with the one obtained in ref.[33] where a completely different approach was taken without relying on the validity of Wick's theorem.

The use of Wick's theorem immediately tells us that $\langle\prod_{i=1}^M\ e^{ik_iX}(z_i)\rangle^N_{\sigma(t_0)}$ should have the following form in terms of $\mathcal{G}^N$.

$$\begin{aligned} &\langle\prod_{i=1}^M\ e^{ik_iX}(z_i)\rangle^N_{\sigma(t_0)} \\ &= \frac{\langle\prod_{i=1}^M\ e^{ik_iX}(z_i)\ \sigma^+(t_0)\ \sigma^-(-t_0)\rangle}{\langle\sigma^+(t_0)\ \sigma^-(-t_0)\rangle} \\ &= \eta(x_0,\vec{k})\ \exp\left(-\frac{1}{2}\sum_{i=1}^M k_i^2\mathcal{G}^N_R(z_i,z_i,t_0) - \sum_{1\le i<j\le M} k_ik_j\mathcal{G}^N(z_i,z_j)\right), \end{aligned} \tag{B.16}$$

where $\vec{k}$ is an M-dimensional vector with k_i's as components and x_0 is the D.b.c of X on $|t| \geq t_0$. $\eta(x_0, \vec{k})$ is a prefactor which is not fixed by Wick's theorem. We will determine $\eta(x_0, \vec{k})$ by using path integral arguments. The second term in the exponential is contributed by the contractions between $X(z_i)$'s for different i's and the first term comes from the self-contractions. $\mathcal{G}_R^N$ is the renormalized self-contraction which has to be defined with a specific regularization procedure. In the following we will first discuss this regularization procedure to define $\mathcal{G}_R^N(z_i, z_i, t_0)$ and then discuss the path integral argument to determine $\eta(x_0, \vec{k})$.

Let us go back to the normalized two point function $\mathcal{G}^N(z, w, t_0)$ in eq.(B.14). Expanding the expression in powers of $(w - z)$ one can readily check that the short distance singularity of $\mathcal{G}^N(z, w, t_0)$ is $-2\ \ln(w - z)$. This is the same as that of the free theory i.e. when the σ operators are absent. This is because locally the theory is always either N.b.c. or D.b.c. (depending on where the region is chosen on the real line) for both of which the short distance singularity is the above one. In the free theory one subtracts this singularity to regularize the self-contraction. We should choose the same regularization in the presence of σ operators also. This choice gives the following renormalized self-contracted two point function:

$$\begin{aligned} \mathcal{G}_R^N(z, z, t_0) &\equiv \lim_{\delta \to 0} \left[\mathcal{G}^N(z, z + \delta, t_0) \ + \ 2 \ln \delta \right] \\ &= -2\ \ln \left[\frac{t_0}{2(t_0^2 - z^2)} \right] \end{aligned} \tag{B.17}$$

Now we will determine the prefactor $\eta(x_0, \vec{k})$. In path integral language we replace the σ operators by constraining the field X to obey the proper boundary conditions on the real axis while integrating over the paths. With $z = \exp(\tau + i\sigma)$ we have the following restriction:

$$\begin{aligned} &X(\tau, \sigma)|_{\sigma=0,\pi} = x_0, \qquad && e^\tau > t_0, \\ &\partial_\sigma X(\tau, \sigma)|_{\sigma=0,\pi} = 0, \qquad && e^\tau < t_0. \end{aligned} \tag{B.18}$$

The basic object that one defines for computing correlation functions in path integral method is the following generating functional,

$$Z[J] = \left\langle \exp\left(i \int d\tau d\sigma J(\tau, \sigma) X(\tau, \sigma) \right) \right\rangle . \tag{B.19}$$

The standard way of computing this [37] is by expanding X by the complete set of

orthonormal eigenfunctions of the Laplacian operator ∇,

$$X(\tau,\sigma) = \sum_I \tilde{x}_I \ \chi_I(\tau,\sigma). \tag{B.20}$$

One performs integrations over $\tilde{x}_I$'s while computing the path integral. Note that χ_0 corresponding to the zero eigenvalue is a constant but $\chi_I(\tau,\sigma)$, for $I \neq 0$ are τ dependent. Hence from eq.(B.18) we can write,

$$\chi_I(\tau,\sigma)|_{\sigma=0,\pi} = 0, \qquad\qquad e^\tau > t_0, \ I \neq 0. \tag{B.21}$$

Therefore for the Dirichlet regions we have from eq.(B.18),

$$X(\tau,\sigma)|_{\sigma=0,\pi} = \sum_I \chi_I(\tau,\sigma)|_{\sigma=0,\pi} = \tilde{x}_0\chi_0 = x_0, \tag{B.22}$$

which means that $\tilde{x}_0$ is non-dynamical and is restricted to be x_0/χ_0. This restriction can be taken into account by inserting $\delta(\tilde{x}_0 - x_0/\chi_0)$ into the path integral. With this the $\tilde{x}_0$ integral in $Z[J]$ becomes,

$$\begin{aligned} Z[J] \ &\rightarrow \ \int d\tilde{x}_0 \ \delta(\tilde{x}_0 - x_0/\chi_0) \ \exp\left(i\tilde{x}_0\chi_0 \int d\tau d\sigma J(\tau,\sigma)\right) \\ &= \exp\left(ix_0 \int d\tau d\sigma J(\tau,\sigma)\right). \end{aligned} \tag{B.23}$$

To compute the correlation function in eq.(B.16) one substitutes $J(\tau,\sigma) = \sum_{i=1}^M k_i \ \delta(\tau - \tau_i) \ \delta(\sigma - \sigma_i)$ which immediately suggests the following[11]:

$$\eta(x_0,\vec{k}) = \exp(ix_0 \sum_{i=1}^M k_i). \tag{B.24}$$

Therefore using eqs. (B.16), (B.17) and (B.24) one gets for $x_0 = 0$,

$$\langle e^{ipX}(0)\rangle_{\sigma(t_0)} = (2t_0)^{-p^2-1/8}, \tag{B.25}$$

which was used in the third equation of (3.24).

Now we will show that the result obtained above for $\langle\prod_{i=1}^M \ e^{ik_iX}(z_i)\rangle_{\sigma(t_0)}^N$ (eqs. (B.16), (B.17), (B.24)) is consistent with the one obtained in ref.[33]. In this work the computation was made with D.b.c. on $\mathbf{R}_{>0}$ and N.b.c. on $\mathbf{R}_{<0}$ i.e. $\sigma^\pm$ were placed at $t = 0$ and $t = -\infty$ respectively. Let us call this $\tilde{z}$ plane. We will be interested in the result on z plane where

[11] Any other part of the prefactor cancels off in a normalized correlation function.

$\sigma^{\pm}$ are placed at $\pm t_0$. These two planes can be connected by an $\mathbf{SL}(2,\mathbf{R})$ transformation which we choose to be the following,

$$\tilde{z}(z) = t_0 \ \frac{z - t_0}{z + t_0}. \tag{B.26}$$

Let us then quote the result from ref.[33]:

$$\langle\sigma| \ \prod_{i=1}^{M} \ e^{ik_i X}(\tilde{z}_i) \ |\sigma\rangle = \kappa(x_0, \vec{k}) \ \prod_{i=1}^{M} (\tilde{z}_i)^{-k_i^2} \ \prod_{1\le i<j\le M} \ \left(\frac{\sqrt{\tilde{z}_i} - \sqrt{\tilde{z}_j}}{\sqrt{\tilde{z}_i} + \sqrt{\tilde{z}_j}}\right)^{2k_i k_j}, \tag{B.27}$$

where $|\sigma\rangle \equiv \sigma^+(0) \ |0\rangle$, $\langle\sigma| \equiv \lim_{u\to 0}\langle 0|I\circ\sigma^-(u) = \lim_{u\to 0} u^{-1/8} \ \langle 0|\sigma^-(-1/u)$ with $|0\rangle$ being the $\mathbf{SL}(2,\mathbf{R})$ invariant vacuum and $I(u) \equiv -1/u$ being the inversion map. In ref.[33] the above expression was found as a solution of a set of first order differential equations (called twisted Knizhnik-Zamolodchikov equation) with respect to $\tilde{z}_i$'s. Therefore the integration constant $\kappa(x_0, \vec{k})$ remained undetermined. We will start from eq.(B.27) and apply the conformal transformation eq.(B.26) to find the expression for $\langle\prod_{i=1}^{M} \ e^{ik_i X}(z_i)\rangle^N_{\sigma(t_0)}$. We use the standard rule for the conformal transformation of a correlation function of primary operators.

$$\begin{aligned}
&\langle\sigma|\prod_{i=1}^{M} \ e^{ik_i X}(\tilde{z}_i)|\sigma\rangle \\
&= \lim_{u,v\to 0} \ u^{-1/8} \ \langle\sigma(-1/u) \ \prod_{i=1}^{M} \ e^{ik_i X}(\tilde{z}_i) \ \sigma(v)\rangle \\
&= \lim_{u,v\to 0} \ u^{-1/8} \ (\tilde{z}'(-1/u) \ \tilde{z}'(v))^{-1/16} \ \prod_{i=1}^{M} (\tilde{z}'(\tilde{z}_i))^{-k_i^2} \\
&\quad \langle\sigma(z(-1/u)) \ \prod_{i=1}^{M} \ e^{ik_i X}(z_i) \ \sigma(z(v))\rangle,
\end{aligned} \tag{B.28}$$

where $\tilde{z}'(\tilde{z}) \equiv \dfrac{d\tilde{z}}{dz}$ expressed in terms of $\tilde{z}$ i.e. $\tilde{z}'(\tilde{z}) = \dfrac{(\tilde{z} - t_0)^2}{2t_0^2}$. $z_i \equiv z(\tilde{z}_i)$. $z(\tilde{z})$ is the inverse function of $\tilde{z}(z)$ (eq.(B.26)), namely $z(\tilde{z}) = -t_0 \ \dfrac{\tilde{z} + t_0}{\tilde{z} - t_0}$. Using these and eq.(B.27) and taking the limit $u, v \to 0$ we get from eq.(B.28),

$$\langle\prod_{i=1}^{M} \ e^{ik_i X}(z_i)\rangle_{\sigma(t_0)} = \kappa(x_0, \vec{k}) \ (2t_0)^{-1/8} \prod_{i=1}^{M} \left(\frac{\tilde{z}_i'}{\tilde{z}_i}\right)^{k_i^2} \ \prod_{1\le i<j\le M} \ \left(\frac{\sqrt{\tilde{z}_i} - \sqrt{\tilde{z}_j}}{\sqrt{\tilde{z}_i} + \sqrt{\tilde{z}_j}}\right)^{2k_i k_j}. \tag{B.29}$$

Therefore the corresponding normalized correlation function will be,

$$\langle \prod_{i=1}^{M} e^{ik_i X}(z_i)\rangle^N_{\sigma(t_0)} = \kappa(x_0,\vec{k}) \prod_{i=1}^{M} \left(\frac{\tilde{z}_i'}{\tilde{z}_i}\right)^{k_i^2} \prod_{1\le i<j\le M} \left(\frac{\sqrt{\tilde{z}_i}-\sqrt{\tilde{z}_j}}{\sqrt{\tilde{z}_i}+\sqrt{\tilde{z}_j}}\right)^{2k_ik_j} . \quad \text{(B.30)}$$

Now using eqs.(B.30, B.14, B.17, B.26) it is straightforward to show that,

$$\begin{aligned}&\langle \prod_{i=1}^{M} e^{ik_i X}(z_i)\rangle^N_{\sigma(t_0)} \\ &= 4^{(\vec{k})^2}\ \kappa(x_0,\vec{k})\ \exp\left(-\frac{1}{2}\sum_{i=1}^{M} k_i^2 \mathcal{G}^N_R(z_i,z_i,t_0) - \sum_{1\le i<j\le M} k_ik_j\mathcal{G}^N(z_i,z_j)\right), \quad \text{(B.31)}\end{aligned}$$

which is the same result as eq.(B.16) with,

$$\kappa(x_0,\vec{k}) = 4^{-(\vec{k})^2}\ \exp(ix_0\sum_{i=1}^{M} k_i). \quad \text{(B.32)}$$

Acknowledgement: It is a great pleasure to thank Ashoke Sen for many useful discussions and guiding suggestions at various stages of this work. Special thanks to Justin David for many stimulating discussions and encouragements. I would also like to thank Ian Ellwood for discussions on numerical analysis. I would like to acknowledge the hospitality of the Institute for Theoretical Physics, Santa Barbara where part of the work was done.

This research was supported in part by the National Science Foundation under Grant No. PHY99-07949.

References

[1] A. Sen, "Universality of the tachyon potential," JHEP **9912**, 027 (1999) [hep-th/9911116].

[2] E. Witten, "Non-Commutative Geometry And String Field Theory", Nucl. Phys. **B268** 253 (1986).

[3] N. Berkovits, "Super-Poincare Invariant Superstring Field Theory", Nucl. Phys. **B450** (1995) 90, [hep-th/9503099].

[4] V. A. Kostelecky and S. Samuel, "On A Nonperturbative Vacuum For The Open Bosonic String", Nucl. Phys. B **336**, 263 (1990).

[5] A. Sen and B. Zwiebach, "Tachyon Condensation in String Field Theory", JHEP **0003**, 002 (2000) [hep-th/9912249].

[6] N. Moeller and W. Taylor, "Level truncation and the tachyon in open bosonic string field theory", Nucl. Phys. **B583**, 105 (2000) [hep-th/0002237].

[7] J.A. Harvey and P. Kraus, "D-Branes as unstable lumps in bosonic open string field theory", JHEP **0004**, 012 (2000) [hep-th/0002117].

[8] R. de Mello Koch, A. Jevicki, M. Mihailescu and R. Tatar, "Lumps and p-branes in open string field theory", Phys. Lett. **B482**, 249 (2000) [hep-th/0003031].

[9] N. Moeller, A. Sen and B. Zwiebach, "D-branes as tachyon lumps in string field theory", hep-th/0005036.

[10] L. Rastelli and B. Zwiebach, "Tachyon potentials, star products and universality", hep-th/0006240.

[11] A. Sen and B. Zwiebach, "Large marginal deformations in string field theory", JHEP **0010**, 009 (2000) [hep-th/0007153].

[12] W. Taylor, "Mass generation from tachyon condensation for vector fields on D-branes", JHEP **0008**, 038 (2000) [hep-th/0008033].

[13] R. de Mello Koch and J.P. Rodrigues, "Lumps in level truncated open string field theory", hep-th/0008053.

[14] N. Moeller, "Codimension two lump solutions in string field theory and tachyonic theories", hep-th/0008101.

[15] H. Hata and S. Shinohara, "BRST invariance of the non-perturbative vacuum in bosonic open string field theory". JHEP **0009**, 035 (2000) [hep-th/0009105].

[16] B. Zwiebach, "Trimming the Tachyon String Field with SU(1,1)", hep-th/0010190.

[17] M. Schnabl, "Constraints on the tachyon condensate from anomalous symmetries", hep-th/0011238.

[18] P. Mukhopadhyay and A. Sen, "Test of Siegel gauge for the lump solution", hep-th/0101014.

[19] H. Hata and S. Teraguchi, "Test of the Absence of Kinetic Terms around the Tachyon Vacuum in Cubic String Field Theory", hep-th/0101162.

[20] I. Ellwood and W. Taylor, "Open string field theory without open strings", hep-th/0103085.

[21] B. Feng, Y. He and N. Moeller, "Testing the uniqueness of the open bosonic string field theory vacuum", hep-th/0103103.

[22] K. Ohmori, "A review on tachyon condensation in open string field theories", hep-th/0102085.

[23] I. Ellwood, B. Feng, Y. He and N. Moeller, "The identity string field and the tachyon vacuum", hep-th/0105024.

[24] L. Rastelli, A. Sen and B. Zwiebach, "String field theory around the tachyon vacuum", hep-th/0012251.

[25] L. Rastelli, A. Sen and B. Zwiebach, "Classical solutions in string field theory around the tachyon vacuum," hep-th/0102112.

[26] L. Rastelli, A. Sen and B. Zwiebach, "Half-strings, Projectors, and Multiple D-branes in Vacuum String Field Theory", hep-th/0105058.

[27] L. Rastelli, A. Sen and B. Zwiebach, "Boundary CFT construction of D-branes in vacuum string field theory," hep-th/0105168.

[28] D. J. Gross and W. Taylor, "Split string field theory. I," JHEP **0108**, 009 (2001) [hep-th/0105059].

[29] D. J. Gross and W. Taylor, "Split string field theory. II," JHEP **0108**, 010 (2001) [hep-th/0106036].

[30] S. Samuel, "The Ghost Vertex In E. Witten's String Field Theory," Phys. Lett. B **181**, 255 (1986).

[31] D. J. Gross and A. Jevicki, "Operator Formulation Of Interacting String Field Theory," Nucl. Phys. B **283**, 1 (1987).

[32] D. J. Gross and A. Jevicki, "Operator Formulation Of Interacting String Field Theory. 2," Nucl. Phys. B **287**, 225 (1987).

[33] J. Frohlich, O. Grandjean, A. Recknagel and V. Schomerus, "Fundamental strings in Dp-Dq brane systems," Nucl. Phys. B **583**, 381 (2000) [hep-th/9912079].

[34] A. LeClair, M. E. Peskin and C. R. Preitschopf, "String Field Theory On The Conformal Plane. 1. Kinematical Principles," Nucl. Phys. B **317**, 411 (1989).

[35] A. LeClair, M. E. Peskin and C. R. Preitschopf, "String Field Theory On The Conformal Plane. 2. Generalized Gluing," Nucl. Phys. B **317**, 464 (1989).

[36] A. Hashimoto, "Dynamics of Dirichlet-Neumann open strings on D-branes," Nucl. Phys. B **496**, 243 (1997) [hep-th/9608127].

[37] See for example, J. Polchinski, "String Theory", Vol. 1.